A new primate community from the earliest Oligocene of the Atlantic margin of Northwest Africa: Systematic, paleobiogeographic and paleoenvironmental implications

Laurent Marivaux, Mohamed Benammi, Lahssen Baidder, Omar Saddiqi, Sylvain Adnet, Anne-Lise Charruault, Rodolphe Tabuce, Johan Yans, Mouloud Benammi

Journal of Human Evolution (https://doi.org/10.1016/j.jhevol.2024.103548)

A new primate community from the earliest Oligocene of the Atlantic margin of Northwest Africa: Systematic, paleobiogeographic and paleoenvironmental implications

Laurent Marivaux [a,] *, Mohamed Benammi [b], Lahssen Baidder [c], Omar Saddiqi [c], Sylvain Adnet [a], Anne-Lise Charruault [a], Rodolphe Tabuce [a], Johan Yans [d] and Mouloud Benammi [e]

[a] *Laboratoire de Paléontologie, Institut des Sciences de l'Évolution de Montpellier (ISE-M, UMR 5554, CNRS/UM/IRD/EPHE), c.c. 064, Université de Montpellier, place Eugène Bataillon, F-34095 Montpellier Cedex 05, France*

[b] *Département de Géologie, Faculté des Sciences, Université IBN Tofaïl, BP 133, 14000 Kénitra, Morocco*

[c] *Laboratoire Géosciences, Faculté des Sciences Aïn Chock, Université Hassan-II-Casablanca, BP 5366 Maârif, 20100 Casablanca, Morocco*

[d] *Departement of Geology, Institute of Life Earth and Environment (ILEE), Université de Namur, rue de Bruxelles 61, 5000 Namur, Belgium*

[e] *Laboratoire Paléontologie Évolution Paléoécosystèmes Paléoprimatologie (PALEVOPRIM, UMR-CNRS 7262), Université de Poitiers UFR SFA, 6 Rue Michel Brunet, F-86022 Poitiers Cedex, France*

* Corresponding author.

E-mail address: Laurent.Marivaux@UMontpellier.fr (L. Marivaux)

ORCID numbers (available):

Laurent Marivaux: 0000-0002-2882-0874

Mohamed Benammi: 0000-0001-6959-700X

Lahssen Baidder: 0000-0001-5318-7102

Omar Saddiqi: 0000-0003-3139-0403

Sylvain Adnet: 0000-0001-7188-1560

Rodolphe Tabuce: 0000-0002-4713-3981

Johan Yans: 0000-0001-7590-0298

Mouloud Benammi: 0000-0003-4707-7518

Abstract

We report a new Paleogene primate community discovered in the uppermost part of the Samlat Formation outcropping on the continental shore of the *Rio de Oro*, east of the Dakhla peninsula (in the south of Morocco, near the northern border of Mauritania). Fossils consist of isolated teeth, which were extracted by wet screening of estuarine sediments (DAK C_2) dating from the earliest Oligocene (ca. 33.5 Ma). These dental remains testify to the presence of at least eight primate species, documenting distinct families, four of which are among the Anthropoidea (Oligopithecidae [*Catopithecus* aff. *browni*], Propliopithecidae [?*Propliopithecus* sp.], Parapithecidae [*Abuqatrania* cf. *basiodontos*], and Afrotarsiidae [*Afrotarsius* sp.]) and four in the Strepsirrhini (a Djebelemuridae [cf. '*Anchomomys*' *milleri*], a Galagidae [*Wadilemur* cf. *elegans*], a possible lorisiform [*Orogalago saintexuperyi* gen. et sp. nov.], and a strepsirrhine of indeterminate affinities [*Orolemur mermozi* gen. et sp. nov.]). This record of various primates at Dakhla represents the first Oligocene primate community from Northwest Africa, especially from the Atlantic margin of that landmass. Considering primates plus rodents (especially hystricognaths), the taxonomic proximity at the generic (even specific) level between DAK C_2 (Dakhla) and the famous Egyptian fossil-bearing localities of the Jebel Qatrani Formation (Fayum Depression), either dating from the latest Eocene (L-41) or from the early Oligocene, suggests the existence of an east-west 'trans-North African' environmental continuum during the latest Eocene–earliest Oligocene time interval. The particularly diverse mammal fauna from DAK C_2, recorded within the time window of global climate deterioration characterizing the Eocene/Oligocene transition, suggests that this tropical region of northwest Africa was seemingly less affected, if at all, by the cooling and associated paleoenvironmental and biotic changes documented at that time, or at least that the effects were delayed. The expected densely forested paleoenvironment bordering the western margin of North Africa at the beginning of the early Oligocene probably offered better tropical refugia than higher latitudes or more inland areas during the cooling episode.

Keywords: Anthropoidea; Strepsirrhini; Tropical North Africa; Atlantic Sahara; Paleogene; Eocene/Oligocene transition

1. Introduction

The evolutionary history of primates in Africa has always attracted much attention. Regardless of the 'recent' emergence of our own family, the early history of primates on this landmass remains a fascinating topic. Although incomplete, the fossil record of Afro-Arabia documenting the early Cenozoic (Paleogene) proves that this landmass was at that time an epicenter of primate diversification, not only of anthropoids, but also of strepsirrhines. The antiquity of the group in Afro-Arabia can be traced back to the dawn of the Cenozoic era, with the still enigmatic *Altiatlasius* from the latest Paleocene of Morocco (Sigé et al., 1990). This taxon, known by about ten isolated teeth is so far the oldest primatomorphan from Afro-Arabia, but its primitiveness makes it difficult to elucidate its phylogenetic status (e.g., Sigé et al., 1990; Hooker et al., 1999; Beard, 2004; Marivaux, 2006; Seiffert et al., 2010; Seiffert, 2012; Ni et al., 2013). From our current knowledge of the Afro-Arabian fossil record, the Paleogene evolutionary histories of subsequent strepsirrhine and anthropoid primates are primarily documented from North Africa, particularly and historically from Egypt (Fayum Depression; for a summary see Seiffert, 2012) but also from Algeria (de Bonis et al., 1988; Godinot and Mahboubi, 1992, 1994; Tabuce et al., 2009), Libya (Jaeger et al., 2010; Beard et al., 2016; Mattingly et al., 2021), Morocco (Gheerbrant et al., 1998; Tabuce et al., 2005) and Tunisia (Hartenberger and Marandat, 1992; Marivaux et al., 2013, 2014), as well as from Arabia (Oman: Thomas et al., 1988, 1991; Gheerbrant et al., 1993, 1995; Saudi Arabia: Zalmout et al., 2010), and to a lesser extent from Sub-Saharan Africa (Kenya: Leakey et al., 1995; Ducrocq et al., 2011; Tanzania: Stevens et al., 2013; Angola: Pickford, 1986; Namibia: Pickford et al., 2008; Godinot et al., 2018). The fragmentary nature of some of these early African primates (e.g., *Azibius*, *Algeripithecus*, '*Tabelia*', '*Dralestes*', *Djebelemur*, *Afrotarsius*, '*Anchomomys*', *Plesiopithecus, Notnamaia*) has led to much confusion about their phylogenetic status, which have been in a state of flux over time between their initial discoveries and the contribution of new data resulting from renewed field efforts (e.g., Sudre, 1975; Simons and Bown, 1985; Simons, 1992; Godinot and Mahboubi, 1992, 1994; Court, 1993; Hartenberger and Marandat, 1992; Simons and Rasmussen, 1994; Simons et al., 1994; Kay et al., 1997; Tabuce et al., 2004, 2009; Godinot, 2006, 2010; Pickford et al., 2008; Jaeger et al., 2010; Marivaux et al., 2013; Gunnell et al., 2018). To date, strepsirrhines are known from a few taxa as early as the late early Eocene (50–45 Ma, Algeria and Tunisia; e.g., Tabuce et al., 2009; Marivaux et al., 2013), while there is so far no evidence for the presence of anthropoids in Africa at the beginning of the Paleogene period (except if we consider the possible anthropoid status of *Altiatlasius*; for a summary see Seiffert, 2012). The earliest known fossil occurrence of anthropoids in Africa dates back only to the end of the middle Eocene epoch (ca. 39.5 Ma), but this record remains very poorly documented to date (Tunisia; Marivaux et al., 2014, 2023). In contrast, the late Eocene–early Oligocene time interval reveals an astonishing diversity of primates, including both strepsirrhines and anthropoids, primarily reflecting the remarkable fossil record of the tropical regions of

northeastern and northern Africa (chiefly Egypt, but also Libya and Algeria) and Arabia (Oman for the early Oligocene) (see Seiffert, 2012). For West Africa and Sub-Saharan Africa, it has so far remained difficult to establish the pattern of primate diversity during the latter time interval, due to the limited number of suitable outcrops and/or, when available, difficulties of access. Here we report a new Paleogene primate community from the western margin of North Africa.

The fossils were unearthed from geological outcrops of the Samlat Formation, which is exposed in the westernmost part of the Sahara, on the continental shore of the *Rio de Oro*, east of the Dakhla peninsula (in the south of Morocco, near the northern border of Mauritania; Fig. 1). In this area, specifically in the sectors of Porto Rico (Pto) and El Argoub (Arg), the uppermost part of the stratigraphical sequence, referred to as Unit 4 (U4 in Benammi et al., 2019), is formed by estuarine deposits dating from the earliest Oligocene (ca. 33.5 Ma; Noiret et al., 2017; Benammi et al., 2019). In 2013, our geological and paleontological surveys at the base of that lithological unit of the Pto and Arg sections have allowed for the discovery of a level (Dakhla C_2 [DAK C_2]) that yielded similar fossil assemblages of marine and estuarine invertebrates (bivalves) and vertebrates (including fishes, turtles, crocodiles, and abundant elasmobranchs; Adnet et al., 2017, 'in prep.'; Benammi et al., 2019), together with terrestrial mammals (Benammi et al., 2019). Among the latter, rodents are abundant and diverse, comprising members of two phylogenetically distinct groups: the Hystricognathi (at least seven species; Marivaux et al., 2017a, 2019) and Anomaluroidea (five species; Marivaux et al., 2017b, 2019). Afrotherians are also represented and illustrated by several 'saghatheriid' hyracoids (including a species of *Saghatherium*) and a herodotiine macroscelid (*Herodotius* aff. *pattersoni*), as well as by a proboscidean, as attested by tooth enamel fragments for the latter (work in progress). Twenty-two isolated teeth in various stages of preservation (including moderately to very worn/corroded/abraded or broken specimens, as well as pristine ones) testify to the presence of at least eight primate species, documenting distinct families, four of which are among the Anthropoidea (Oligopithecidae, Propliopithecidae, Parapithecidae, and Afrotarsiidae) and four in the Strepsirrhini (Djebelemuridae, Galagidae, a possible representative of the lorisiforms, and a strepsirrhine of indeterminate affinities). This record of various primates from the earliest Oligocene of Dakhla represents the first Oligocene primate community from Northwest Africa, especially from the Atlantic margin of that landmass. Here we describe the taxa of this new primate fauna and compare them with their sub-contemporaneous counterparts from northern and northeastern Afro-Arabia (Egypt, Libya, and Oman) and Sub-Saharan Africa (Kenya). We then discuss the paleobiogeographic and paleoenvironmental implications of that discovery at the scale of North Africa, and particularly in the context of the global cooling (and its corollaries) recorded at the Eocene/Oligocene transition (e.g., Berggren and Prothero, 1992; Coxall and Pearson, 2007; Zanazzi et al., 2007; Westerhold et al., 2020).

2. Materials and methods

2.1 Fossil recovery and extraction

The primate-yielding localities of Porto Rico U4 level C_2 (DAK-Pto C_2) and El Argoub U4 level C_2 (DAK-Arg C_2) consist of unconsolidated sandy microconglomerates with a thickness of ~30 cm (Fig. 1). We excavated and collected a total of about five tons of sediment of this level (ca. 2500 kg in each spot) over five successive field seasons (2013–2023). Gross sediments were processed by wet screening (three mesh sizes of sieves; 6 mm, 2 mm, and 1 mm) directly into the seawater of the *Rio de Oro*. The coarse residues from the screening (≥ 2 mm) were carefully scrutinized by eye *in situ*, in order to collect medium-sized fossil elements. The fine residues (1 mm ≤ fossils < 2 mm) were generally screened/washed twice, dried, and then observed under a stereomicroscope in the field and in the laboratory. The fossil material consists primarily of bone fragments and tens of isolated teeth, among which the dental specimens of primates reported here.

2.2 Fossil repository

The fossil material described in this paper is temporarily housed in the paleontological collections of the *Université de Poitiers* (*Laboratoire Paléontologie Évolution Paléoécosystèmes Paléoprimatologie* [PALEVOPRIM]), France. It will be subsequently housed permanently at the *Université IBN Tofaïl*, Kénitra, Morocco.

2.3 High-resolution µCT scan

The three-dimensional (3D) data presented in this work were produced through the technical facilities of Montpellier RIO Imaging (ISE-M, Montpellier, France). We used X-ray microtomography (µCT scans) to obtain 3D digital models (3D surface renderings) of the fossil teeth (Figs. 3–6). Each specimen was scanned with a resolution of 6 µm using a µCT-scanning station EasyTom 150 / Rx Solutions. The crown and roots of each tooth were virtually delimited by manual segmentation under AVIZO 2020.2 (Visualization Sciences Group). The teeth were prepared within a 'Label Field' module of AVIZO, using the segmentation threshold selection tool. The 3D digital models of the tooth surface of the different primates described in this paper are available on MorphoMuseuM (Marivaux et al., 2024), an online open access platform that aims to enhance accessibility to 3D models (http://morphomuseum.com).

2.4 Dental loci, nomenclature and measurements

The terminology for the primate dentition (Fig. 2) follows Marivaux et al. (2023) and the literature cited therein. Teeth were measured (maximum mesiodistal length [MDL] and

maximum buccolingual width [BLW]) on the 3D digital models, using AVIZO 2020.2 measurement tools (Table 1).

2.5 Body mass estimation

Whenever possible, estimates of adult body masses (BM) were predicted using regression equations provided by Egi et al. (2004), based on premolar and molar areas (maximum MDL times maximum BLW; Table 1). For anthropoids from DAK C_2, BM estimates were calculated from the anthropoid equations depending on available dental loci. Similarly, BM estimates for strepsirrhines recorded in DAK C_2 were calculated from the 'prosimian' equations depending on available dental loci. A correction for logarithmic transformation bias, known as the ratio estimator (RE; Smith, 1993), was applied to each adult BM estimate as the predicted BM times the RE (see Egi et al., 2004: table 2).

3. Systematic paleontology

Class Mammalia Linnaeus, 1758

Order Primates Linnaeus, 1758

Suborder Haplorhini Pocock, 1918

Infraorder Anthropoidea Mivart, 1864

Family Oligopithecidae Kay and Williams, 1994

Genus *Catopithecus* Simons, 1989

Type species *Catopithecus browni* Simons, 1989

Catopithecus aff. *browni*

Studied specimens DAK-Arg-087, right M_3 (Fig. 3A–B); DAK-Arg-088, right M_2 (Fig. 3C–D); DAK-Arg-089, left M_1 (Fig. 3E–F); DAK-Pto-052, right M_1 (Fig. 3G–H); DAK-Arg-090, left P^4 (Fig. 3I–J); DAK-Arg-091, left M^2 (Fig. 3K–L); DAK-Pto-053, right M^1 (Fig. 3M–P).

Localities Dakhla, El Argoub U4 level C_2 (DAK-Arg C_2) and Porto Rico U4 level C_2 (DAK-Pto C_2), Atlantic margin of North-Saharan Africa (Fig. 1).

Formation and age Upper Samlat Formation, earliest Oligocene (earliest Rupelian; Benammi et al., 2019).

Description Teeth documenting this taxon are so far the most abundant among primate dental remains recovered from DAK C_2 (Fig. 3A–P). The lower molars available (M_1, M_2, and

M_3; Fig. 3A–H) are characterized by a very broad, wide talonid, while their trigonids are reduced and pinched mesiodistally. The trigonid basin is slightly higher than the talonid basin. The trigonid is dominated by the protoconid and metaconid, which are of equal size in all teeth. There is only a trace of a paraconid, the latter being vestigial on all three dental loci (Fig. 3A–H), appearing as a very small, low enamel swelling on the mesial margin of the crowns, located at equal distance from the protoconid and metaconid, and connected to the lingual extremity of a slightly arched, low paracristid. However, judging the development of this mesial cuspid is somewhat difficult, given the degree of abrasion (Fig. 3A–B) or breakage (Fig. 3E) in this region of the trigonid on available specimens. Despite the corrosion of the enamel surface on most specimens, there does not appear to be any strong development of the premetacristid, the latter being absent on the pristine DAK-Pto-052 M_1 (Fig. 3G–H), thereby leaving the trigonid open lingually. The distal trigonid wall is closed by the strong development of the protocristid, which connects to the buccal aspect of the metaconid. On the pristine DAK-Pto-052 M_1, the protocristid is gently sloping towards the flank of the metaconid (Fig. 3G). The talonid bears three equally-sized main cuspids (hypoconid, entoconid, and hypoconulid). On M_1 and M_2, the hypoconulid occupies a distolingual position, almost twinned with the entoconid. Only a very narrow, shallow notch separates the two cuspids (as seen particularly on the DAK-Pto-052 M_1; Fig. 3G). With wear, the two cuspids form a distolingual platform (Fig. 3C–F). On M_3, the hypoconulid is distally displaced, but preserves its lingual position, being connected to the entoconid via a long and well-defined postentocristid (Fig. 3A). On this distal lower dental locus, the breadth of the talonid is similar to that of the trigonid, whereas on M_2 and M_1, the trigonid is markedly narrower than the talonid due to a more buccal position of the hypoconid with respect to the protoconid (this character being accentuated on M_1; Fig. 3E). The hypoconid and entoconid are aligned along a buccolingual axis, whereas the metaconid is slightly more distally positioned to the protoconid (notably on M_1). Lingually, the talonid basin is closed by the development and junction of short pre-entocristid and postmetacristid. The latter are not strongly elevated and slope gently from the entoconid and metaconid, respectively, giving the lingual wall of the talonid a U-shape in lateral perspective. On the pristine DAK-Pto-052 M_1, the connection between the postmetacristid and the pre-entocristid is not fully achieved, resulting in a very thin notch on the lingual wall of the talonid (Fig. 3H). Distally, the hypocristid is strong, extends from the hypoconid to the hypoconulid, and forms the distal crown margin of the three dental loci. Buccally, the cristid obliqua is also strong and trenchant on the three loci, connecting the hypoconid to the trigonid wall at a point distal to the protoconid. In the immediate vicinity of the protoconid, the cristid obliqua runs part way up the distal flank of this cuspid (Fig. 3B, D, F). On M_2 and M_3, the hypoflexid is very shallow, or even non-existent (Fig. 3A–D), whereas on M_1 it may be more pronounced, but still shallow (Fig. 3E–F). There is no pronounced development of a buccal cingulid (except a trace limited to the area between the protoconid and the hypoconid on the DAK-Arg-089 M_1; Fig. 3E–F), and thus the hypoconid and protoconid are marginally situated. The same is true for the metaconid and the

entoconid-hypoconulid complex on the lingual margin. The five main cuspids are not basally inflated, thereby making the buccal and lingual crown margins particularly steep-sided.

The upper teeth available (P^4, M^1, and M^2; Fig. 3I–P) have a transverse crown outline (i.e., much wider than they are long), with salient main cusps. On molars, there is neither internal conules nor well-defined buccal styles. For the latter structures, the inferred absence is based on observation of the worn M^2 (Fig. 3K–L), inasmuch as the M^1, although much less worn, lacks a part of its buccal crown margin due to a break (Fig. 3M). However, the presence of a parastyle on this M^1 cannot be excluded, given the large surface of breakage, located directly mesial to the half-preserved paracone. On M^1 and M^2, the paracone and metacone are virtually aligned along a mesiodistal axis. Moderately high but sharp postparacrista and premetacrista, extend gently sloping from the apex of the paracone and metacone, respectively, and are aligned along a mesiodistal axis. They link the two buccal cusps, thereby closing the trigon basin buccally. The protocone of these molars is mesially canted and lingually bordered by a strong, complete lingual cingulum. The latter extends anteriorly and posteriorly to form a short mesial cingulum and a long distal cingulum, respectively. The mesial cingulum tapers buccally, ending its course at mid-crown width, at the level where a paraconule would normally occur. The distal cingulum expands buccally, ending at the base of the distal flank of the metacone. On both molars, the lingual part of the distal cingulum displays a small, barely discernible enamel swelling, suggesting the possible presence of a tiny hypocone. Only on M^2, the lingual cingulum bears another noticeable enamel swelling (associated to a small dentine pit due to attritional wear) located directly lingual to the protocone, thereby indicating the presence of a small pericone on that specimen. M^1 and M^2 also differ in the shape of their distal crown margin, which is moderately invaginated on M^1 (Fig. 3M), whereas it is buccolingually straight on M^2 (Fig. 3K). On M^2, which preserves its buccal margin, there is a thin but well-defined buccal cingulum, clearly visible between the paracone and the metacone. This cingulum extends mesially at the base of the buccal aspect of the paracone, but tapers off, ending at the mesial base of the paracone (where a parastyle could occur if the crown was not damaged at this point). It is not developed in the buccal region of the metacone. Lingually, the protocone of M^1 and M^2 displays well-defined, long, mesiobuccally and distobuccally oriented pre- and post-protocone cristae (wide-open U-shaped protocone cristae; Fig. 3K, M), which circumscribe a wide trigon basin. The preprotocrista extends mesiobuccally, sloping gently from the apex of the protocone up the location where a paraconule would normally occur (it is absent), then continues buccally beyond that point (via the preparaconule crista) to reach the mesial extremity of a very short preparacrista (on M^1, this mesial crest could be connected buccally to a parastyle; Fig. 3M–O). A long, strong hypoparacrista arises from the lingual flank of the paracone, extends lingually in a gentle slope (Fig. 3N, P), and turns sharply mesially at the midline of the tooth to connect to the preprotocrista (this description comes from M^1, as this dental trait is not clearly observable on M^2 due to enamel abrasion in this occlusal area). Distally and parallel to the hypoparacrista, a similarly developed hypometacrista (well-marked on M^1; Fig. 3M, P) arises

at mid-slope of the lingual flank of the metacone, extends lingually, and connects to the distobuccal extremity (ending abruptly) of the postprotocrista.

The single upper premolar recovered and (tentatively) associated with this taxon is a P^4 (Fig. 3I–J). This tooth is transverse, distinctly narrow, oval to rectangular in occlusal outline, and compatible in size with the upper molars described above. It is bicuspid, primarily dominated by a strong, tall and acute paracone on the buccal region of the crown, and a relatively small, somewhat 'crestiform' protocone in the lingual region. These two main cusps are widely spaced buccolingually from each other. The protocone is particularly canted mesially, clearly more anterior than the paracone on a buccolingual axis, and appears as a small, acute enamel swelling on the mesiolingual margin of the crown. In lingual view (Fig. 3J), the paracone is triangular in shape, with only slightly developed but sharp pre- and post-paracone cristae, both connecting small styles located at the base of the mesial and distal flanks of that main buccal cusp. The buccal flank of the paracone is particularly steep-sided, with a barely visible cingulum at its base. In contrast, its lingual flank is gently sloping. Although there are some traces of corrosion in the lingual region of the crown, there is, however no sign of lingual, mesial and distal cingulum development, unlike the two upper molars which bear strong cingula. The distolingual flank of the protocone is bulging and gently sloping. Only the pre- and post- protocone cristae are developed, and constitute the mesial, lingual and distal margin of the crown. Both protocone cristae extend buccally and connect to the styles situated on either side of the paracone. A discrete (very short and low) hypoparacrista can be seen, connecting the mesiolingual base of the paracone to the preprotocrista.

Comparisons The set of lower molars described here from DAK C_2, display a wide talonid basin with respect to the reduced, short trigonid basin, the latter being slightly taller than the talonid. They have their main cuspids marginally positioned on steep-sided buccal and lingual crown margins, exhibit a well-defined hypoconulid occupying a lingual position and twinned with the entoconid (on M_1 and M_2), lack strong development of a buccal cingulid, and display a reduced, very low paraconid. Associated upper molars exhibit strong lingual (complete), mesial (short) and distal (long) cingula; a buccal cingulum weakly expressed; some degree of invagination of the distal crown margin; well-marked hypoparacrista and hypometacrista; strong, wide-open U-shaped protocone cristae; a minute to absent hypocone, and lack conules. This suite of dental traits characterizes oligopithecids from North Africa, such as *Catopithecus* (*C. browni*; Egypt, Fayum L-41, latest Eocene; Simons, 1989, 1990, 1995a; Simons and Rasmussen, 1996), *Oligopithecus* (*O. savagei*; Egypt, Fayum Quarry E, early Oligocene; Simons, 1962; Rasmussen and Simons, 1988) and *Talahpithecus* (*T. parvus*; Libya, Dur At-Talah DT-Loc. 1, late Eocene; Jaeger et al., 2010), and from Arabia (*Oligopithecus rogeri*; Oman, Taqah, early Oligocene; Gheerbrant et al., 1995). On the upper molars of DAK C_2, the distal crown margins are moderately waisted and their lingual cingulum bears tiny enamel swellings testifying to the presence of minute hypocone and pericone cusps. These features on the upper molars suggest affinities with *Catopithecus* and *Talahpithecus* rather

than with *Oligopithecus*, in which upper molars have a distal crown margin much more waisted (deeply invaginated), and their lingual cingulum (strong and complete in *O. rogeri* [see Gheerbrant et al., 1995, fig. 1a]; strong but somewhat incomplete in *O. savagei* [e.g., Rasmussen and Simons, 1988, fig. 1]) shows no trace of hypocone or pericone development. The dental material from DAK C_2 is, however, more compatible with *Catopithecus* than with *Talahpithecus* (the fossil record of which is very limited; Jaeger et al., 2010), in which the cusps and cuspids are less bulbous and rather acute, the crests and cristids less developed and rather thin, and the cingula much less strong.

The morphology of the DAK-Arg-090 P^4 is also more in line with that of the P^4 of *Catopithecus* and *Talahpithecus* than with that of *Oligopithecus*. In the latter case, notably in *O. rogeri* (see Gheerbrant et al., 1995, fig. 1a), the P^4 displays a more rectangular outline, bears a very strong lingual cingulum that extends, as on its molars, mesiobuccally and distobuccally up to the midline (i.e., presence of strong mesial and distal cingula, respectively), and exhibits a long and strong hypoparacrista. In *O. savagei* (see Rasmussen and Simons, 1988, fig. 2), the P^4 is more sub-triangular, displays strong pre- and post- paracristae, well-marked lingual and distal cingula (mesial cingulum absent), and does not show any hypoparacrista development. The P^4 of *Talahpithecus parvus* (see Jaeger et al., 2010, fig. 2o) is clearly triangular due to a lesser mesiodistal extension of the protocone and the total absence of the cingula in the lingual region of the crown, and it does not show any development of a hypoparacrista. The P^4 of *Catopithecus browni* (see Simons, 1989, fig. 4; Simons and Rasmussen, 1996, fig. 9) has a more oval to sub-triangular outline, more like DAK-Arg-090, but unlike the latter, it shows stronger development of the styles (particularly the parastyle) and the presence, albeit moderately developed, of the lingual and distal cingula, the mesial cingulum being virtually absent. The DAK-Arg-090 P^4 is somewhat unique in having a very small, "crestiform" protocone that is clearly placed mesially (associated with a long, arched postprotocrista), a feature also observed on the P^4 of *Catopithecus* and *Talahpithecus*, but to a lesser extent, whereas on the P^4 of *Oligopithecus*, the protocone is clearly stronger and occupies a central position, aligned with the paracone along a buccolingual axis. To some extent, the DAK-Arg-090 P^4 can also be compared with the isolated P^4 attributed to *Nosmips* (*N. aenigmaticus*; Egypt, Fayum BQ-2, early late Eocene; Seiffert et al., 2010, fig. 1H), an enigmatic primate whose phylogenetic position is unclear. On the latter, as on DAK-Arg-090, there is no cingulum development in the lingual region of the crown, whereas the buccal cingulum is better marked than on the DAK C_2 specimen. Unlike DAK-Arg-090, the *Nosmips*' P^4 has slightly waisted mesial and distal crown margins, and displays a larger protocone that is less mesially positioned (more aligned with the paracone on a buccolingual axis), bearing only a short postprotocrista (not as extensively long and arched as on DAK-Arg-090).

Based on molar size, the oligopithecid from DAK C_2 is about twice the size of *Talahpithecus parvus*, about a quarter larger than *Catopithecus browni*, and about one-third smaller than *Oligopithecus* (*O. savagei* and *O. rogeri*). Given its greater affinity with *Catopithecus* than with *Talahpithecus* and *Oligopithecus*, we then attribute this dental

material from DAK C_2 to *Catopithecus*. There are few morphological distinctions between the DAK C_2 dental specimens and the teeth of *C. browni*. However, given the size difference, we prefer to provide here an assignment with open nomenclature (i.e., *C.* aff. *browni*), instead of formally referring these dental remains to *C. browni*. As shown above, the morphology of the DAK-Arg-090 P^4 does not entirely correspond to that of the P^4 of *Catopithecus*. It also bears some resemblance with the P^4 attributed to *Nosmips*. For these reasons, we only tentatively refer this specimen from DAK C_2 to *C.* aff. *browni*. It cannot be ruled out that this tooth could document a taxon other than *Catopithecus*; another alpha taxonomic option that requires more dental material then current data allow. Body mass predictions calculated from different dental loci reveal a wide range of estimated weights for this taxon (920–2060 g; Table 1), certainly reflecting a sampling of teeth from several individuals of slightly different sizes. It is also possible that for some specimens, the degree of abrasion and corrosion has altered the linear measurements (i.e., loss of surface volume), and consequently the body mass estimates.

Family Propliopithecidae Strauss, 1961

Genus *Propliopithecus* Schlösser, 1910

?*Propliopithecus* sp.

Studied specimen DAK-Pto-056, right M_3 (fragment of talonid; Fig. 3Q–S).

Locality Dakhla, Porto Rico U4 level C_2 (DAK-Pto C_2), Atlantic margin of North-Saharan Africa (Fig. 1).

Formation and age Upper Samlat Formation, earliest Oligocene (earliest Rupelian; Benammi et al., 2019).

Description The only tooth recovered of this primate taxon is a fragment of lower molar which, although partial, corresponds to the largest primate specimen found from DAK C_2. It consists of a portion of talonid preserving the lingual and distal crown margins bearing a well-defined entoconid, an accessory smaller cuspid situated directly distobuccal to the entoconid, and a conspicuous hypoconulid (Fig. 3Q). Mesiolingually, half of the metaconid is also preserved, and buccally, only a part of the lingual aspect of the hypoconid is preserved. The entoconid is aligned with the hypoconid along a buccolingual axis, and with the metaconid along the mesiodistal axis. Although the metaconid and hypoconid are incomplete, their preserved parts indicate that both cuspids were much larger and taller than the entoconid. The latter and the hypoconulid have a similar elevation (Fig. 3R–S), but the hypoconulid is prominently developed (bulbous). This large hypoconulid is situated far distally with respect to the entoconid and hypoconid, and occupies a midline position. It forms a well-defined but moderately sized distal heel, which remains clearly narrower than the maximum buccolingual breadth of the talonid. Lingually, the entoconid displays a short and gently sloping pre-

entocristid, which almost reaches the distal extremity of a short, low, somewhat cuspid-like postmetacristid. The lingual margin of the talonid is therefore practically walled off, with only a very low and narrow notch between the pre-entocristid and the postmetacristid. The postentocristid is very short, almost non-existent. Over the entire length that the postentocristid would normally occupy, a small, well-defined accessory cuspulid (i.e., *tuberculum sextum*) is developed between the entoconid and the hypoconulid. Due to the presence of this accessory cuspid, there is no distolingual fovea, and the margin of the talonid basin is thus closed distolingually. Only a deep but very narrow notch between the postentocristid and the accessory cuspid incises the distolingual talonid margin. Buccally, the hypocristid is moderately developed and weakly trenchant. There is no distobuccal fovea. The development and position of the main cuspids with respect to each other, generating a vast, unobstructed talonid basin, the oval (rather than rectangular) outline of the crown with a mesiodistal long axis, and the absence of an interstitial contact facet on the distal aspect of the hypoconulid, point to this lower tooth being a third molar (M_3). Moreover, the pristine condition of this unrooted tooth, with acute cuspids without any attritional wear, indicates that this M_3 was unerupted, i.e., it was still enclosed in its bony crypt inside the dentary.

Comparisons The fragmentary nature of the DAK-Pto-056 specimen does not allow us to observe a number of characters, such as the presence or absence of a strong buccal cingulid, the development and position of the cristid obliqua, and the configuration of the trigonid, which are particularly diagnostic of lower molars of the large anthropoids of this epoch in Afro-Arabia, i.e., early Oligocene Propliopithecidae (*Aegyptopithecus*, *Moeripithecus*, and *Propliopithecus*; e.g., Schlösser, 1910, 1911; Simons, 1965; Kay et al., 1981; Simons et al., 1987; Thomas et al., 1991). However, the preserved crown portion of the DAK-Pto-056 M_3 has a lingual margin relatively straight-sided (rather than being strongly basally inflated as in *Aegyptopithecus* and *Moeripithecus*), with acute cuspids marginally situated, and the development of an accessory distolingual cuspid, which are dental traits observed, to some extent, on the lower molars of most species of *Propliopithecus* (e.g., Kay et al., 1981; Seiffert et al., 2010). Despite the specimen being only a fragment, its estimated maximum length and width (deriving from our tentative reconstruction of the missing tooth part; Fig. 3Q) would indicate that the size of this tooth was close to that of the M_3 of *Propliopithecus haeckeli* (based on the unique mandibular specimen documenting this species; Schlösser, 1910, 1911; Kay et al., 1981). Although the dimensions of that dental locus (M_3) can vary from one individual to another within a species (e.g., Kay et al., 1981), based on these estimated dimensions, this propliopithecid from DAK-Pto C_2 was almost one-third smaller than *Propliopithecus chirobates*, *Propliopithecus ankeli* and *Moeripithecus markgrafi*, and twice as small as the large *Aegyptopithecus zeuxis*.

Family Parapithecidae Schlösser, 1911

Genus *Abuqatrania* Simons, Seiffert, Chatrath and Attia, 2001

Type species *Abuqatrania basiodontos* Simons, Seiffert, Chatrath and Attia, 2001

Abuqatrania cf. *basiodontos*

Studied specimens DAK-Arg-094, left M^1 or M^2 (corroded, lacking the enamel cap; Fig. 4A–B); DAK-Arg-101, left M^3 (Fig. 4C–D); DAK-Arg-095, right I_1 or I_2 (Fig. 4E–I); DAK-Arg-093, a right M_1 (Fig. 4J–M); DAK-Arg-096, right P_2 (Fig. 4N–R); DAK-Arg-097, right P_2 (Fig. 4S–V); DAK-Arg-092, left C_1 (Fig. 4W–A').

Locality Dakhla, El Argoub U4 level C_2 (DAK-Arg C_2), Atlantic margin of North-Saharan Africa (Fig. 1).

Formation and age Upper Samlat Formation, earliest Oligocene (earliest Rupelian; Benammi et al., 2019).

Description Seven isolated teeth (two upper and five lower) were recovered and attributed to this taxon due to their compatible size and morphology. The DAK-Arg-094 upper molar is severely corroded, to the extent that the enamel cap has been entirely lost (Fig. 4A–B). The dentine is exposed and provides the underlying occlusal morphology of this tooth. It will therefore be difficult to make precise comparisons, as we have lost the volume of the occlusal enamel surface. However, despite the absence of enamel, the main structures of the occlusal surface can be identified and, to a certain extent, appreciated via the remanent relief of the enamel-dentine junction (EDJ). We can thus observe three main, large tubercles, which are the paracone, metacone and protocone, and three secondary, smaller tubercles, which are the hypocone and two conules. The two latter consist of a moderately developed but well-defined paraconule, and a stronger, conspicuous metaconule. The apices of these cups and conules are truncated due to attritional wear that was somewhat advanced. These tubercle apices must have appeared as dentine pits before the loss of the covering enamel layer. Based on the relief of the dentine surface, it may be expected that the tooth was relatively bunodont with moderately bulbous cusps and conules, and without significant crest development. Only a trace of a short hypometacrista can be observed between the lingual base of the metacone and the strong metaconule. A small spur is also visible in the mesiolingual region of the metaconule, corresponding to a small, short crest that may be either a postprotocrista or a hypometaconule crista. Paracone and metacone are aligned along a mesiodistal axis, and the protocone is mesially canted. The hypocone appears slightly lingual to the protocone and located far distally from the latter, without any trace of connection crests (absence of prehypocrista). The dentine reliefs of the paracone and metacone are merged, virtually twinned (8-shaped structure), thereby suggesting that the

two buccal cusps were relatively close together, with their sides coalescing (distal flank of the paracone and mesial flank of the metacone merged, or perhaps postparacrista and premetacrista merged). The lingual flank of the paraconule is merged with the mesiobuccal flank of the protocone. At this stage, there is no indication of the presence of a preprotocrista. In contrast, a thin preparaconule crista is barely visible, extending buccally from the paraconule to a point mesial to the paracone. We cannot judge whether or not a parastyle is present where the preparaconule crista would end its course. The dentine bulge observable at the base and around almost the entire crown outline (except directly mesial to the paracone and paraconule, and also directly distal to the metacone), indicates the presence of mesial, lingual, distolingual (including the hypocone) and distal enamel cingula, likely well-marked and continuous. In contrast, the buccal cingulum was probably more discreet. The distal crown margin of this tooth shows no invagination, and is strictly rectilinear along the buccolingual axis. In contrast, the mesial margin is more angular, with a mesiodistal constriction of the lingual region.

The DAK-Arg-101 M^3 is in a better state of preservation, albeit abraded on its mesiobuccal aspect (Fig. 4C–D). It has three roots, a large lingual root and two slender buccal roots (mesial and distal). The distal buccal root is very small and lingually displaced, almost below the mesial buccal root (Fig. 4D). The occlusal pattern of that M^3 corroborates the morphological expectations made on the corroded DAK-Arg-094 M^2, in particular the moderately bulbous condition of the main cusps, the weak (or absence of) development of crests, and the presence of well-marked mesial, lingual and distal cingula. This M^3 has two main cusps, the protocone and the paracone, which are aligned along a buccolingual axis (Fig. 4C). A very small but well-defined metacone is also visible, abutting the paracone, and occupying a much more lingual position (distolingual to the paracone). It bears a short premetacrista that ends subsumed in the distal flank of the paracone (or the postparacrista, barely visible). Although damaged mesially, it seems that a paraconule is present associated with a preparaconule crista extending buccally, and tapering to disappear at the base of the mesial flank of the paracone. The mesial cingulum is particularly well marked, forming a full-fledged enamel fold extending from the lingual aspect of the protocone to the level of the paraconule. The lingual cingulum is more discreet but well defined, and continues distally then buccally to form the distal crown margin. There is no trace of a hypocone in its distolingual part. The distal cingulum ends buccally, at a point distal to the minute metacone. The buccal cingulum is faintly distinguishable due to abrasion.

Lower teeth available consist of a well-preserved, virtually pristine M_1 (Fig. 4J–M), two damaged P_2 (Fig. 4N–V), a canine in good condition (Fig. 4W–A'), and a worn incisor (I_1 or I_2; Fig. 4E–I). The DAK-Arg-093 M_1 is bunodont but with moderately bulbous not strongly inflated cuspids, showing thin, low but well-defined inter-cuspid cristids (Fig. 4J). The trigonid is narrow but long, smaller than the talonid in occlusal area, and slightly more elevated (Fig. 4K). The metaconid is clearly located distally to the protoconid on a buccolingual axis, and the two cuspids, equally sized, are joined by a thin, low but complete protocristid (not notched),

which forms the distal wall of the trigonid (Fig. 4L–M). The mesialmost part of the crown bears a well-defined cuspidate paraconid that is almost twice as small as the protoconid and metaconid. This paraconid is more buccal to the metaconid on a mesiodistal axis (Fig. 4J), but far distant from the latter, almost midway between the protoconid and metaconid. The relative positions of the three main trigonid cuspids form a perfect equilateral triangle. The protoconid and paraconid are connected by a thin, low paracristid. Lingually, there is no premetacristid development, and thus the trigonid remains widely open lingually. The talonid bears three equally-sized main cuspids (entoconid, hypoconid, and hypoconulid; Fig. 4J–K). The entoconid is aligned with the hypoconid along a buccolingual axis, and with the metaconid along a mesiodistal axis. The entoconid and metaconid are relatively close due to the very posterior position of the metaconid. The talonid basin is closed lingually, but the lingual wall is deeply indented, appearing as a narrow V-shaped notch formed by the short, steeply sloping postmetacristid and pre-entocristid (Fig. 4K). The hypoconid is distinctly more buccal than the protoconid (talonid width greater than trigonid width). Distally, the hypoconulid is slightly lingual to the midline, close to the entoconid but not strongly twinned with it; a deep notch separates the two cuspids. There is no distolingual fovea. The hypoconulid displays a short, gently sloping buccal cristid, which joins the short postcristid arising from the hypoconid (i.e., hypocristid). There is a well-defined distobuccal cingulid, which runs part way up the distal flank of the hypoconid, ending at the junction between the hypoconulid cristid and the hypocristid (Fig. 4J–L). There is no cingulid at the base of the buccal aspect of the hypoconid. Only a faint enamel bulge can be seen at the base of the buccal aspect of the protoconid, and on its mesial base, extending up to the base of the paraconid, thereby indicating the presence of a very discrete buccal to mesiobuccal cingulid (Fig. 4J–K). The buccal crown margin is waisted (invaginated) due to the confluence of the bases of the hypoconid and protoconid, and the lack of development of a strong buccal cingulid. The cristid obliqua runs mesially from the apex of the hypoconid up to the base of the trigonid wall, ending at a point slightly distolingual to the protoconid. It does not extend up the distal protoconid flank (Fig. 4J–L). The hypoflexid is shallow, somewhat accentuated by the more buccal position of the hypoconid relative to the protoconid.

The two P_2 (Fig. 4N–R and 4S–V) are tiny, single-rooted teeth. DAK-Arg-096 preserves almost the entire root shaft (Fig. 4O–R), whereas on DAK-Arg-097, the root has been broken off just below the cervix. On DAK-Arg-096, the root appears strongly compressed mesiodistally (similar in width to the crown, and half the length of the crown). At the collar, the root appears constricted, due to the presence of a cingulid at the base of the crown, developed around the entire periphery. This cingulid is far more pronounced lingually, where it appears as a full-fledged enamel fold, whereas buccally it appears as a discrete enamel bulge at the base of the crown. The crown is dominated by a single cuspid, the protoconid, which is prominent and very tall. On both P_2 specimens, the apex of the protoconid is truncated due to attritional wear. This prominent cuspid displays a well-defined, curved and sloping paracristid which appears as a mesial winglet. There is no trace of paraconid in its mesiolingual region. The paracristid merges seamlessly with the lingual cingulid. Distally, at

the junction of the well-marked lingual cingulid and the faint buccal cingulid, there is a noticeable enamel swelling, which could correspond to a small metaconid or hypoconid. This tiny cuspid-like swelling is more visible on DAK-Arg-096 (Fig. 4P, R) than on DAK-Arg-097, in which this part of the crown is partially damaged (Fig. 4U). There is no trace of connection between this small cuspid-like swelling and the protoconid.

The DAK-Arg-092 canine (C_1; Fig. 4W–A') has a rounded oval cross-section, being moderately compressed buccolingually (mesiodistal long axis). It is particularly well preserved, showing only a few traces of attritional wear at the apex of its main, protruding cuspid and on its distolingual aspect. The root is massive and slightly curved inwards, almost twice as high as the crown, and it tapers in its distal part. The crown is unicuspid, formed by a tall and pointed protoconid, which likely projected well above the protoconids of $P_{2\text{-}4}$. From a lateral perspective and in a vertical plane, the buccal flank of the protoconid is markedly curved (small radius of curvature), so much so that its apex is almost vertically aligned with the base of the distal margin of the crown (Fig. 4A'). The protoconid displays a moderately developed paracristid, which is oblique (steep) to the occlusal plane. The base of the crown has a strong, unbroken lingual cingulid and a faint, incomplete buccal cingulid. The lingual cingulid runs from a large distal heel to the mesial terminus of the paracristid. The distal aspect of the protoconid bears a distal cristid extending from the truncated apex of the cuspid up to the distal lingual cingulid (at the level of the heel). This cristid is worn away by attrition and appears as a narrow, shallow groove (flat-bottomed) along the distal flank of the protoconid. It does not bisect the lingual cingulid.

DAK-Arg-095 is a first or second lower incisor (I_1 or I_2; Fig. 4E–I). The crown cross-sectional shape is rounded oval (Fig. 4E). The crown apex is worn by attrition, but the remaining part is clearly wider mesiodistally than the root, with an occlusal edge orthogonal to the long axis of the root, thereby giving this incisor a spatulate shape (Fig. 4F). Its root is strongly mesiodistally compressed (buccolingual long axis). Based on the ratio of incisor over molar occlusal crown surfaces (I_x/M_1 # 0.35), this lower incisor can be described as moderately small in proportion to the post-canine teeth (incisor size classification; e.g., Ross et al., 1998; Kay et al., 2004), and given the crown shape (although part of the crown is missing), this tooth could be interpreted as low crowned. There is no apparent occlusal cuspid, and the mesial and distal edges are continuous and rounded. The lingual crown surface bears a central, vertically oriented pillar of enamel that is flanked both mesially and distally by shallow concavities (Fig. 4E–F). On the center of the pillar, a tiny, circular enamel cuspulid can be observed, but there is no formal identification of this structure, which is atypical (perhaps pathological?). The buccal crown outline is gently curved (convex) in lateral perspective (Fig. 4I). There is no buccal cingulid. Although somewhat obscured by wear, a faint but complete lingual cingulid can be observed. The lingualmost edge of this cingulid is slightly bulged that could indicate the presence of small heel.

Comparisons We have assembled here a set of isolated dental specimens that are compatible both in size and morphology. Not all teeth have the same degree of preservation (including a

heavily corroded upper molar without its enamel cap), but all share a moderate bunodonty, characterized by slightly basally inflated cusps and cuspids (main or secondary), and by low, weakly developed crests and cristids. Among the best-preserved specimens, the DAK-Arg-093 lower molar reveals a number of anatomical details, which are primarily found in early parapithecids from Africa (such as *Biretia*, *Abuqatrania*, or *Qatrania*; e.g., de Bonis et al., 1988; Simons and Kay, 1983, 1988; Simons et al., 2001; Seiffert et al., 2005a; Jaeger et al., 2010). Indeed, in addition to its moderate bunodonty, this lower molar from DAK C_2 has a trigonid basin that is relatively higher than the talonid basin, displays a small but well-defined paraconid (twice as small as the protoconid and metaconid), and lacks a premetacristid (trigonid open lingually). Its talonid is short with a conspicuous hypoconulid that occupies a position close to the entoconid but not twinned to the latter (nearly centrally placed, situated slightly lingual to midline, and separated from the entoconid by a well-marked notch), and has a weak, low and short cristid obliqua. The DAK-Arg-093 tooth is interpreted as a M_1 due to the position of the metaconid, which is markedly situated distal to the protoconid, as well as the position of the paraconid, which is located far distant from the metaconid and more buccal than the latter, and due to the orientation of the crista obliqua, which meets the base of the trigonid wall, slightly lingual to the protoconid. The overall appearance and structural pattern of the DAK-Arg-093 M_1 is particularly reminiscent to that of the M_1 preserved on the CGM 42841 mandible (bearing P_4–M_3), holotype of *Abuqatrania basiodontos* (see Simons et al., 2001). This early parapithecid is known from the latest Eocene of Egypt (Fayum, L-41). The size of the DAK-Arg-093 M_1 is also similar to that of the CGM 42841 M_1. On the latter, the cuspids are bulbous, becoming more so distally along the toothrow; a feature that we are unable to assess due to the lack of material from Dakhla (M_2 and M_3 are not yet documented at DAK C_2). Comparisons with *Abuqatrania* are unfortunately limited to the M_1, as the latter taxon is known only by its lower dentition (P_4–M_3), its lower anterior dentition (I_1–P_3) being undocumented, as is its entire upper dentition. The same applies to *Qatrania* from Egypt, younger than *Abuqatrania* by around 1 Ma (Fayum Quarry M and Quarry E, *Qatrania fleaglei* and *Qatrania wingi*, respectively; early Oligocene, see Simons and Kay, 1988). *Qatrania* is morphologically very close to *Abuqatrania*, and is also primarily known from its lower dentition, its upper dentition being documented only by a partial upper molar (*Q. wingi*; Beard and Coster, 2016; Seiffert et al., 2020). Lower molars of *Qatrania* have slightly more bulbous cuspids than those of *Abuqatrania*. The cuspids are otherwise well defined, particularly well delimited and isolated by deep, very narrow notches. The DAK-Arg-093 M_1 as well as M_1 of *Abuqatrania* do not show such deep and narrow inter-cuspid delimitations, and have their trigonid noticeably narrower than their talonid, a condition that is not as marked on the M_1s of *Qatrania*, notably *Q. wingi* (e.g., Simons and Kay, 1988, figs 2–4; Beard, 2002, fig. 9.9). The cristid obliqua of the DAK-Arg-093 M_1 as well as on M_1 of *Abuqatrania* is less oblique, reaching the base of the distal trigonid wall, slightly lingual to the protoconid, and not near the buccal flank of the metaconid as it does on the M_1s of *Q. fleaglei* and *Q. wingi*.

Although the DAK-Arg-094 upper molar (M^1 or M^2) is heavily corroded, without enamel cap, its remnant relief (EDJ) provides some information on its occlusal pattern that can be

compared with that of the only known upper half-molar referred to as *Q. wingi* (Beard and Coster, 2016). DAK-Arg-094 is transversely broad and bore (judging from the marked EDJ relief) a moderately developed but well-defined hypocone as well as conspicuous conules, moderate lingual and buccal cingula, closely spaced paracone and metacone, and seemingly had only weak development of the transverse crests (i.e., moderately bunodont). Although we do not have access to the volume of the occlusal structure that the enamel layer could provide, it does appear that DAK-Arg-094 was less bunodont (i.e., cups less inflated) than the condition characterizing the upper molar of *Qatrania*. On the latter, the mesial and lingual cingula are particularly prominently developed, with a strong pericone situated directly lingual to the protocone. The cingula were most likely weakly marked on DAK-Arg-094, and no EDJ relief is observed in the lingual region of the tooth, thereby suggesting the absence of a pericone. Due to the presence of a strong mesial cingulum, the upper molar of *Qatrania* has a more rectangular lingual outline than DAK-Arg-094, the lingual region of which is constricted mesiodistally.

The occlusal morphology of the DAK-Arg-094 upper molar would in fact be more in line with that characterizing the upper molars of *Biretia*. This genus is the oldest known representative of the Parapithecidae in Africa. It is documented from the early late Eocene of Algeria (Bir el-Ater, *Biretia piveteaui*; de Bonis et al., 1988), Egypt (Fayum BQ-2, *Biretia megalopsis* and *Biretia fayumensis*; Seiffert et al., 2005a) and Libya (Dur At-Talah DT-Loc-1, *B. piveteaui*; Jaeger et al., 2010). Upper molars of the different species of *Biretia* are moderately bunodont, without significant development of inter-cusp transverse and longitudinal crests. As on DAK-Arg-094 (deduced from the EDJ occlusal relief), lingual, mesial and distal cingula are well marked on upper molars of *Biretia*, forming full-fledged enamel folds/shelfs, with a well-developed but not inflated hypocone in the distolingual region, and without any trace of pericone in the mesiolingual region; unlike the derived conditions observed on the upper molar of *Qatrania*. The upper molars of *Biretia* show no distal invagination, and their margins are rectilinear along a buccolingual axis, as is particularly expressed on DAK-Arg-094. Unlike *Abuqatrania* and *Qatrania*, *Biretia* is also documented by upper M^3s and lower teeth, including premolars (notably a P_2). This record thus provides further morphological insights for comparisons with the DAK C_2 material. Compared with the DAK-Arg-101, the M^3 in *B. megalopsis* (Seiffert et al., 2005a, fig. 2B) has a more rectangular than oval occlusal outline, with a stronger and more buccally positioned metacone, and a long and well-defined hypoparacrista (absent on DAK-Arg-101). In *B. piveteaui*, the M^3 is more oval in shape, like the DAK-Arg-101 specimen, but with a greatly reduced, almost absent metacone (Jaeger et al., 2010, fig. 2q). The protocone of the DAK-Arg-101 M^3 appears larger than on M^3 of *Biretia*. The lingual cingulum seems also less marked than on the M^3 of *Biretia*. Concerning the lower teeth, the M_1s of *Biretia* have a less buccolingually constricted trigonid, as their paraconid occupies a slightly more lingual position, closer to the metaconid than on the DAK-Arg-093 M_1 or on the M_1 of *Abuqatrania*. The trigonid of M_1s in *Biretia* is almost closed lingually, not only due to the position of the paraconid but also to the presence a very short premetacristid, an 'incipient' cristid that is absent on the DAK-Arg-093 M_1 or on the M_1 of *Abuqatrania*. The

talonid basin of M_1s in *Biretia* is also slightly longer and broad, with a stronger and longer development of the cristid obliqua, and a better marked closure of the lingual wall. A small buccal cingulid forming a shelf is present between the protoconid and the hypoconid on lower molars of *Biretia* (especially on M_2 and M_3, but to a lesser extent on M_1), a character that is absent on DAK-Arg-093 and lower molars of *Abuqatrania*. The M_1 of *B. megalopsis* also bears an accessory cuspulid in its distolingual region (i.e., *tuberculum sextum*; Seiffert et al., 2005a, fig. 2E), the latter being absent on M_1 of *B. fayumensis*, as well as on DAK-Arg-093, and on M_1 of *Abuqatrania*. It is worth noting that a similar tubercle development can be observed on the M_2 of *Q. wingi*. Finally, the P_2 in *Biretia* (documented in *B. megalopsis*; Seiffert et al., 2005a, fig. 2F–G) is structurally similar to the DAK-Arg-096 and DAK-Arg-097 identified as P_2s. As in *Biretia*, the latter two specimens from DAK C_2 are single rooted and have a simple crown dominated by a single cuspid, the protoconid, surrounded by a circular cingulid, which is more strongly marked lingually than buccally. The outline of P_2 in *B. megalopsis* is almost rounded, with a gently sloping lingual flank of the protoconid, whereas the two specimens from DAK C_2 are slightly more oval in shape (long mesiodistal axis), with a steeper-sided lingual flank of the protoconid. On the DAK-Arg-096 P_2, there is a noticeable distal enamel swelling, which could correspond to a small metaconid or hypoconid. The latter is not observed on the P_2 of *B. megalopsis*.

Additional comparisons can be made with other parapithecids, such as *Apidium* and *Parapithecus/Simonsius*, which are well known from early Oligocene sites that are younger by around 3 Ma (especially Egypt, Fayum, upper sequence of the Jebel Qatrani Formation, e.g., Osborn, 1908; Schlösser, 1910; Simons, 1962, 1974, 1995b; Seiffert et al., 2010; and Libya, Zallah, Z7I, Beard et al., 2016; Mattingly et al., 2021). The latter taxa are significantly larger, with upper and lower teeth showing a dramatically advanced degree of bunodonty, with strongly inflated cusps, conules and cuspids. Despite a dental pattern of upper molars closely reminiscent to earlier parapithecids (especially *Biretia* and DAK-Arg-094), these taxa have more quadrangular crown outlines, and show variable development of the cingula (either strongly developed with a pericone as in *Apidium*, or variably absent *versus* present as in *Parapithecus*/*Simonsius*). Unlike DAK-Arg-093, lower molars of *Parapithecus*/*Simonsius*, notably M_1s, have no more paraconid, and their trigonids are very constricted mesiodistally and closed lingually due to the presence of a strong, arched premetacristid joining the strong paracristid. There is no longer a protocristid connecting the protoconid to the metaconid, and only the lateral protocristid remains, which is directed distolingually, joining an almost non-existent cristid obliqua. In *Apidium*, lower molars exhibit a more conservative morphology with well-defined, inflated but separated cuspids (no coalescence of cuspid flanks), and often have additional cuspulids, especially in *Apidium bowni* (e.g., centroconid, *tuberculum sextum*, etc.). Whereas a well-defined paraconid is preserved (and almost contiguous with the metaconid) on M_1 of the latter taxon, there is no trace of a paraconid on M_1s of *Apidium phiomense* and *Apidium mustaphai* (e.g., Seiffert et al., 2010; Beard et al., 2016), and their trigonid is very constricted mesiodistally and closed lingually due to the presence of a strong and arched premetacristid joining the strong paracristid. As on lower molars of

Parapithecus/*Simonsius* and unlike DAK-Arg-093, in *Apidium* there is no longer a protocristid connecting the protoconid to the metaconid (presence of a deep notch separating both cuspids), and only an obliquely distolingually oriented lateral protocristid is present, connecting a short cristid obliqua or the centroconid. Lower molars of *Apidium* also display a well-marked buccal cingulid running along the entire length of the crown, and rising lingually on the distal and mesial margins up to the midline. A simpler, distinct version of the lower molar morphology of *Apidium* is exemplified by *Lokonepithecus*, a small parapithecid taxon from the late early Oligocene of Kenya (Lokone Hill, LOK 13; Ducrocq et al., 2011). DAK-Arg-093 differs substantially from the M_1 of *Lokonepithecus* in having a trigonid that is higher and narrower than the talonid, bearing a paraconid, lacking a premetacristid, and preserving a continuous protocristid (complete distal trigonid wall). On the smaller DAK-Arg-93 M_1, the talonid basin remains lingually open (deep V-shaped notch between the metaconid and entoconid), and displays a more buccally positioned cristid obliqua, with no buccal cingulid between the protoconid and the hypoconid.

The dental characteristics of the two upper molars (M^1 or M^2, and M^3) and the lower teeth (M_1, P_2, C_1, and I_1 or I_2) undoubtedly indicate parapithecid affinities of this anthropoid primate from DAK C_2, at least with early parapithecids rather than with more advanced parapithecids or other anthropoids from Africa, such as proteopithecids and oligopithecids (diagnoses of the latter are provided in Seiffert et al., 2010). Comparisons of the material from DAK C_2 suggest more explicitly affinities with *Abuqatrania basiodontos* from L-41, Egypt, particularly with regard to the first lower molar (M_1), the morphology and size of the DAK-Arg-093 M_1 being very close to those of the M_1 of this taxon. Unfortunately, the upper dentition and lower front dentition are not documented for *A*. *basiodontos*. The morphology of upper teeth and lower front teeth from DAK C_2, although not comparable with that of *A*. *basiodontos*, is nevertheless compatible with that characterizing the dentitions of *Biretia*, *Qatrania*, or of more recent parapithecids (*Apidium* and *Parapithecus*/*Simonsius*), as they share a similar dental parapithecid Bauplan. Given the high morphological similarity and size compatibility of DAK-Arg-093 with M_1 of *A. basiodontos*, we assign this dental material from DAK C_2 to *Abuqatrania*, but leave the nomenclature open regarding the alpha taxonomy (i.e., *A.* cf. *basiodontos*), pending further material. In this taxonomic context, our descriptions of the upper teeth and lower front teeth from DAK C_2, thus further our knowledge of the dental morphology of *Abuqatrania*. The contribution of this new dental material from DAK C_2, attributed to this genus, and the morphological differences with the dental material attributed to *Qatrania*, reinforce the validity of the genus *Abuqatrania*. The latter had been placed in synonymy with *Qatrania* (Beard, 2013) because there were virtually no differences in lower dental morphology between *Abuqatrania basiodontos* and *Qatrania wingi* (and only the lower dentition was known at that time). We show here that the lower molars of *Abuqatrania* differ to some extent from those of *Qatrania*, and that the upper molar of DAK C_2, although heavily corroded, shows substantial differences from the unique and partial specimen attributed to *Qatrania*. By adding new fossil material, we then strengthen support for the validity of *Abuqatrania*, because the upper molar morphology of the DAK-Arg-094

specimen is much more primitive than that of the *Qatrania wingi* upper molar fragment described by Beard and Coster (2016).

Family Afrotarsiidae Ginsburg and Mein, 1987

Genus *Afrotarsius* Simons and Bown, 1985

Type species *Afrotarsius chatrathi* Simons and Bown, 1985

Afrotarsius sp.

Studied specimens DAK-Arg-098, left P_3 (Fig. 5A–E); DAK-Pto-054, right M_1 (Fig. 5F–J).

Localities Dakhla, El Argoub U4 level C_2 (DAK-Arg C_2) and Porto Rico U4 level C_2 (DAK-Pto C_2), Atlantic margin of North-Saharan Africa (Fig. 1).

Formation and age Upper Samlat Formation, earliest Oligocene (earliest Rupelian; Benammi et al., 2019).

Description Only two small lower teeth are recognized and associated to document this tiny taxon. They consist of a P_3 (Fig. 5A–E) and a M_1 (Fig. 5F–J), which are both damaged and abraded/corroded. The M_1 is particularly corroded in lacking a part of its enamel layer on the lingual aspect of the tooth, a lack of covering enamel which accentuates the pointed appearance of the residual dentine relief corresponding to the metaconid and entoconid (Fig. 5G, H, J). This molar is double-rooted, with each root arcuate and particularly slender (Fig. 5G–H). The occlusal structure of this tooth is characterized by a wide talonid basin and a smaller but higher trigonid basin (Fig. 5F). The latter is slightly higher and buccolingually narrower than the talonid (Fig. 5G). The metaconid and protoconid are of equal size (considering the lack of enamel layer on the metaconid), virtually aligned along a buccolingual axis, and connected by a complete and trenchant protocristid, thereby closing the distal trigonid wall. A low, barely defined paraconid (not cuspidate) occupies a mesiolingual position, located almost in line with the metaconid on a mesiodistal axis (slightly buccal), but distant, far away mesially from it. This weakly differentiated paraconid is connected to the protoconid via a long, arched paracristid, which forms the mesial margin of the tooth. There is no development of a premetacristid, and thus the trigonid basin remains wide open lingually (V-shaped trigonid). The talonid bears two main cuspids (hypoconid and entoconid), which are buccolingually opposed (aligned). A minute third cuspid, the hypoconulid, faintly developed, can be observed distally (on the distolingual margin), near the entoconid (distobuccal to it), almost twinned to the latter. The entoconid displays a very short postentocristid connected to the hypoconulid, and a long pre-entocristid, which extends mesially, sloping gently to the base of the metaconid (or its short, faintly developed

postmetacristid), thereby closing the talonid basin lingually. However, although walled-off, the latter remains widely indented (flat-U-shaped wall in lateral perspective; Fig. 5G–H). Distally, the hypoconid is connected to the hypoconulid by a straight and trenchant hypocristid. There is neither a distobuccal nor a distolingual fovea. A long and trenchant cristid obliqua connects the hypoconid to the trigonid wall at a point distobuccal to the protoconid. The cristid obliqua runs part way up the distal flank of the protoconid (Fig. 5G, J). Given the very buccal position of the cristid obliqua, there is virtually no hypoflexid. Furthermore, there is no trace of buccal cingulid, and the buccal margin of the crown is thus steep-sided, with the hypoconid, protoconid and cristid obliqua marginally positioned (Fig. 5F–G). On the lingual side, the absence (loss) of the enamel layer hampers appreciation of the shape of the margin, even though the entoconid and metaconid are in a marginal position.

The P_3 is single rooted and simply constructed, with the crown dominated by the protoconid. The root appears particularly massive and long/high (compared to the crown), but shallow grooves, barely visible over the entire height of the buccal (Fig. 5B) and lingual (Fig. 5D–E) aspects of the root shaft, suggest that this single root results from the fusion of two roots (mesial and distal roots merged). The crown is essentially formed by the trigonid. There is no talonid, only a cingulid bordering the base of the distal crown margin. This cingulid is also present but poorly developed buccally, at the very base of the protoconid, and does not extend mesially (Fig. 5B–C). A very small but distinct metaconid can be observed on the distolingual base of the protoconid (Fig. 5A, D–E). This metaconid is clearly lower than the prominent protoconid. A thin, oblique protocristid connects the two cuspids. Mesially, the crown margin is formed by a strong, long, arched paracristid (Fig. 5A, C). The latter bears a minute enamel swelling in its mesiolingual extremity (Fig. 5A, D–E), which could testify to the presence of a tiny, very low paraconid. A discrete lingual cingulid, extending from the paraconid to the distal cingulid bounds the lingual margin of the crown. The buccal flank of the protoconid is steep-sided, while its lingual flank is sloping.

Comparisons Afrotarsiids are so far documented by *Afrotarsius*, known from the late Eocene (*Afrotarsius libycus*, Dur At-Talah DT-Loc. 1, Libya; Jaeger et al., 2010) and early Oligocene (*Afrotarsius chatrathi*, Fayum Quarry M, Egypt; Simons and Bown, 1985) in North Africa, and by its South Asian counterpart, *Afrasia*, known from the late middle Eocene (*Afrasia djijidae*, Pondaung Formation, Myanmar; Chaimanee et al., 2012). These small-bodied taxa are poorly documented, and the DAK C_2 specimens, limited to two lower teeth (P_3 and M_1), do not substantially increase the record of this group. However, lower molars are known for each known species of Afrotarsiidae, and thus comparisons with the single lower molar found at DAK C_2 allow this specimen to be formally identified with this primate group. In addition to its tiny size characteristic of the group, the DAK-Pto-054 M_1 displays a wide talonid basin and a smaller but also wide V-shaped trigonid basin, remaining open lingually and higher than the talonid, as in other afrotarsiids. This lower molar also differs from its homologs in other species of *Afrotarsius* and *Afrasia*, in showing a lesser development of the paraconid (very strong in *Afrasia*), less bulbous main cuspids, and in lacking the development of a complete

buccal cingulid. The molar from DAK C_2 is particularly abraded and corroded, which perhaps artificially removed the presence of this cingulid. DAK-Pto-054 also displays a hypoconulid occupying a slightly more lingual position, with respect to the more mid-line position observed in lower molars of *A. libycus* and *A. chatrathi*. In this respect, the position of the hypoconulid on the DAK C_2 specimen is more similar to that observed on the single molar (M_2) of *Afrasia*. P_3 is only documented in *A. chatrathi*, but in very poor state of preservation, which drastically limits the scope of our comparison with the DAK-Arg-098 P_3. Based on the size/area of the DAK-Pto-054 M_1 (Table 1), this afrotarsiid from DAK C_2 was about one-third smaller than *A. chatrathi*, but roughly the same size as *A. libycus* and *Af. djijidae*. The discovery of upper molars would have enabled a much better identification of the afrotarsiid taxon from DAK C_2, or even the recognition of a possible new species. The lack of fossil material does not allow us to go any further. We recognize the affinities with the genus *Afrotarsius*, but leave the species in open nomenclature (*Afrotarsius* sp.), pending the discovery of additional dental specimens.

Suborder Strepsirrhini Geoffroy Saint-Hilaire, 1812

Family Djebelemuridae Hartenberger and Marandat, 1992 (*sensu* Godinot, 2010)

Genus *Anchomomys* Stehlin, 1916

'*Anchomomys*' *milleri* Simons, 1997

Nomenclatural remark We follow Seiffert et al. (2005b) and Godinot (2006) who consider that this taxon from L-41 (Fayum, Egypt; Simons, 1997) does not belong to *Anchomomys* from Europe (e.g., Stehlin, 1916; Marigó et al., 2011) and requires a new generic designation. Quotation marks are therefore applied here to the genus name ('*Anchomomys*' *milleri*).

cf. '*Anchomomys*' *milleri*

Studied specimen DAK-Arg-100, right C_1 (Fig. 6A–D).

Localities Dakhla, El Argoub U4 level C_2 (DAK-Arg C_2), Atlantic margin of North-Saharan Africa (Fig. 1).

Formation and age Upper Samlat Formation, earliest Oligocene (earliest Rupelian; Benammi et al., 2019).

Description This lower tooth (DAK-Arg-100; Fig. 6A–D) is primarily documented by a well-preserved crown. Its root is broken below the cervix, but the small piece preserved indicates that the root was mesiodistally compressed (oval cross-section), and thus narrower than the crown base (Fig. 6B). The crown appears to be rotated compared to the root orientation, so

that it is oriented along a mesiodistal long axis, while the root is oriented along a buccolingual long axis. The occlusal morphology is simple, characterized by the presence of a single, massive, protruding cuspid, i.e., the protoconid. The latter is slightly buccolingually compressed and adjoined by a strong, very high and mesially oriented paracristid (or preprotocristid). The two merged structures form a blade-shaped main tubercle, projecting anteriorly. The mesial flank of the paracristid is steep-sided and slightly arched in lateral perspective (Fig. 6B–C), extending backwards to the base of the crown, to join a well-marked lingual cingulid. The latter forms a bulge of enamel extending over the entire distolingual margin of the crown. The distal flank of the protoconid is abrupt, bearing a thin, barely visible cristid developed over the entire height of the distal aspect of the protoconid, and merging with the distal cingulid at the base of the crown (Fig. 6D).

Comparison The morphology of this small lower tooth is unusual, characterized by a protruding, sloping blade-shaped protoconid-paracristid complex, relatively procumbent. This very distinctive morphology, however, corresponds in all points to the configuration of the lower canine of '*Anchomomys*' *milleri*, a djebelemurid taxon from the latest Eocene of Egypt (Fayum L-41; Simons, 1997; see also Seiffert et al., 2003, 2005b; Godinot, 2006). This taxon is documented only by a mandible bearing C_1-M_3. With a similar size and identical morphology to the canine of '*A.*' *milleri*, we therefore identify the DAK-Arg-100 isolated tooth as a lower canine. The post-canine teeth of '*A.*' *milleri* also have the distinctive feature of a blade-like protoconid-paracristid complex, which is repeated on the three successive premolars ($P_{2–4}$), as it is also observed in known lower premolars of *Djebelemur martinezi*, another djebelemurid from the late early Eocene of Tunisia (Chambi; Hartenberger and Marandat, 1992; Marivaux et al., 2013). This group of primates (djebelemurids), harboring such a specialized lower front-dentition (C_1–$P_{2–4}$), is recognized and identified as the 'pre-tooth-combed' primates (Godinot, 2006; Marivaux et al., 2013). This blade-shaped morphology of the mesial region of the lower premolars is also observed in a galagid lorisiform, *Wadilemur elegans*, from the latest Eocene of Egypt (Fayum L-41; Simons, 1997; Seiffert et al., 2005b). The lower canine of *Wadilemur* is so far not documented, only its alveolus on the dentary bone, which is greatly reduced and particularly inclined forward. The same applies to the lower incisor alveoli of the same fossil specimen. In addition, the crown of the P_2 in *Wadilemur* is particularly blade-shaped and very procumbent, overlapping the alveolus of the canine. As suggested by Seiffert et al. (2005b), this arrangement of the premolars and the configuration of the canine and incisor alveoli indicate that *Wadilemur* had very reduced and 'styliform' canine and incisors, most certainly like those that characterize the procumbent tooth-comb of lorisiforms and lemuriforms (crown strepsirrhines). The DAK-Arg-100 canine therefore had a different morphology from that expected for *Wadilemur*. Although the size would be compatible, it is for this reason that we do not assign this DAK-Arg-100 canine to *Wadilemur* cf. *elegans*, also recorded at DAK C_2 (see below). We prefer to attribute this unique specimen from DAK C_2 to '*Anchomomys*' *milleri*, whose canine morphology corresponds exactly to that of DAK-Arg-100. Given the extreme rarity of the material, we attribute this lower canine to cf. '*A.*' *milleri* at this stage.

Infraorder Lorisiformes Gregory, 1915

Family Galagidae Gray, 1825

Genus *Wadilemur* Simons, 1997

Type species *Wadilemur elegans* Simons, 1997

Wadilemur cf. *elegans*

Studied specimens DAK-Arg-099, right M_2 (Fig. 6E–I); DAK-Arg-103, right M^1 or M^2 (Fig. 6J–L).

Localities Dakhla, El Argoub U4 level C_2 (DAK-Arg C_2), Atlantic margin of North-Saharan Africa (Fig. 1).

Formation and age Upper Samlat Formation, earliest Oligocene (earliest Rupelian; Benammi et al., 2019).

Description The unique lower molar (DAK-Arg-099; Fig. 6E–I) assigned to this species is more or less rectangular in occlusal outline, being much longer than it is wide. It is characterized by a large trigonid, only slightly shorter and narrower than the talonid, the two basins having virtually the same elevation (Fig. 6F, H). Its occlusal structure comprises four main cuspids, which are acute, almost equal in size and marginally positioned (steep external flanks, slightly swollen at their base). The metaconid is situated far distally to the protoconid on a buccolingual axis (Fig. 6E). The two cuspids are connected by a complete but moderately indented protocristid, which nevertheless closes the trigonid basin distally (Fig. 6E, I). The protoconid displays a long, low and arched paracristid. The latter first extends in a mesial direction (i.e., preprotocristid; Fig. 6E), plunging abruptly from the apex of the protoconid (Fig. 6F–H), then curves sharply and acquires a reverse orientation (i.e., distolingual; Fig. 6E, G–H). It merges with a long, mesially oriented premetacristid, thereby closing the trigonid basin mesiolingually (Fig. 6E, G–H). There is no trace of paraconid in the mesial crown margin (which is occupied solely by the paracristid). The talonid basin appears as a circular bowl (Fig. 6E). The entoconid is barely lower than the hypoconid, and slightly bent lingually (Fig. 6I). The entoconid is a little more distally positioned than the hypoconid on a buccolingual axis (Fig. 6E). It displays two long and sloping arms, the pre- and post- entoconid cristids. Buccally, the hypoconid is a mirror image of the entoconid (symmetrical with respect to the long axis of the midline), also with two long, but much higher and slightly thicker arms, the hypocristid and cristid obliqua. These two main talonid cuspids associated with their arms are mirror-symmetrical with an open U-shaped configuration, and form the distolingual and distobuccal corners of the crown. The postentocristid and hypocristid join and merge near the midline of the crown. There is no sign of hypoconulid. At the junction of these two latter cristids, a flat

area can be seen that extends over a large part of the distal aspect of the crown (Fig. 6E, I), and corresponds to the contact facet with the succeeding tooth (probably the M_3). There is a well-defined distobuccal cingulid, which runs up the distal flank of the hypoconid, ending at the junction between the postentocristid and the hypocristid (Fig. 6E–G, I). There is no cingulid at the base of the buccal flank of the hypoconid, nor between the latter and the protoconid, nor around the latter (absence of buccal cingulid), and thus these two buccal cuspids are marginally situated (Fig. 6E–G). Extending from the hypoconid, the cristid obliqua is long, strong and trenchant, runs mesiolingually and reaches the distal trigonid wall at a point situated between the protoconid and the metaconid (Fig. 6E, G, I). In the vicinity of the trigonid, the cristid obliqua runs part way up the flank of the distal trigonid wall (Fig. 6F–G), but does not reach the top of the protocristid (Fig. 6I). The configuration of the cristid obliqua results in a moderately deep hypoflexid (Fig. 6E–G).

The second dental specimen assigned to this species is a broken upper molar. DAK-Arg-103 is a right M^1 or M^2, which lacks its entire mesial and buccal parts (Fig. 6J–K). The preserved part (corresponding to approximately half the tooth) is somewhat smoothed, but provides information on the configuration and connections of the metacone, protocone and hypocone. Only the distal flanks of the protocone and metacone are preserved, as well as a small portion of the base of the distolingual flank of the paracone (Fig. 6J). These preserved flanks of the three main cusps provide an insight into the size and shape of the trigon basin, which was relatively short and narrow. Although incomplete, the protocone and metacone appear to be of equal size and similar height (based on distal perspective; Fig. 6L). These two cusps are connected by a well-defined and apparent continuous transverse crest, which includes at least a postprotocrista and a hypometacrista. The postprotocrista extends distally from the apex of the protocone. It slopes gently down the distal flank of the protocone, then curves distobuccally towards the metacone. At crown midline, it joins a hypometacrista originating at mid-slope of the lingual flank of the metacone. There is no metaconule on the postprotocrista-hypometacrista complex, nor any small enamel swelling on that crest that might indicate the presence of a vestigial metaconule (Fig. 6J, L). Distobuccally, the metacone displays a strong, long, oblique (distobuccally oriented) postmetacrista. It is difficult to assess whether or not a metastyle is present, as the crown is broken at this point. However, a tiny enamel swelling observable in the distobuccal extremity of the postmetacrista may suggest the presence of this style (Fig. 6J–L). Distolingually, the crown displays a strong cingulum bearing a well-defined and cuspate hypocone, but distinctly lower than the protocone. The hypocone may appear doubled (two twinned cusps), but this is actually the result of a crack that gives the false appearance of a double hypocone (Fig. 6J–K). A short, low but clearly visible prehypocrista connects the mesiobuccal flank of the hypocone to the base of the distal flank of the protocone. The lingual cingulum is almost non-existent, appearing as a barely pronounced bulge of enamel at the base of the lingual flank of the protocone. The distal cingulum is in contrast well developed and appears as a full-fledged low enamel shelf, extending along the entire distal crown margin. It gradually tapers and disappears in the distobuccal region of the crown, below the distal extremity of the postmetacrista. The

metacone is aligned with the hypocone along a buccolingual axis (as could also be the case for the paracone with the protocone, according to our tentative reconstruction of the missing part of the crown, based on homologous dental loci of closely related species; Fig. 6J). Despite the buccolingual alignment of the metacone and hypocone, the development of a long postmetacrista significantly increases the buccal length of the crown relative to the lingual length (although we cannot judge this formally due to the breakage of the tooth), making the crown outline sub-triangular. The distal crown margin of this tooth is markedly waisted (strong invagination at midline) as a result, demarcating the region of the hypocone, which appears as a distolingually protruding lobe.

Comparison The morphology of the DAK-Arg-099 lower molar is in line with that characterizing some stem strepsirrhines from the Paleogene of Afro-Arabia. This is particularly shown by the configuration of its trigonid, which displays a long paracristid oriented mesially (preprotocristid) then retroversely, joining a strong, long premetacristid, and thus closing the trigonid basin lingually. Such a trigonid configuration is indeed found in lower molars of the djebelemurids *Djebelemur martinezi* from the late Early Eocene of Tunisia (Chambi; Hartenberger and Marandat, 1992; Marivaux et al., 2013), '*Anchomomys*' *milleri* from the latest Eocene of Egypt (Fayum L-41; Simons, 1997) and also *Omanodon minor* and *Shizarodon dhofarensis* from the early Oligocene of Oman (Taqah; Gheerbrant et al., 1993), the azibiids *Algeripithecus minutus* and *Azibius trerki* from the late early–early middle Eocene of Algeria (Gour Lazib; e.g., Tabuce et al., 2009), as well as in all other strepsirrhines from the Paleogene of Africa, resolved at the base of the Lorisiformes clade, such as *Wadilemur elegans* from Egypt (Fayum L-41; Simons, 1997; Seiffert et al., 2005b) and three other taxa, *Karanisia arenula* from the late Eocene of Libya (DT-Loc.1, Dur At-Talah; Jaeger et al., 2010), *Karanisia clarki*[1] and *Saharagalago misrensis* from the early late Eocene of Egypt (Fayum BQ-2; Seiffert et al., 2003). The DAK-Arg-099 lower molar lacks, however, the buccal cingulid (notably around the protoconid and the hypoflexid), which is particularly well developed in lower molars of *Djebelemur, Omanodon*, *Shizarodon* and '*A.*' *milleri*, in *Algeripithecus* (to a lesser extent in *Azibius*), and also in *Karanisia* and *Saharagalago*. The DAK-Arg-099 lower molar is further distinguished from lower molars of '*A.*' *milleri*, as well as those of *K. clarki*, in the lack of a small but cuspidate paraconid, which occupies a very buccal position in the latter taxa (almost mesial to the protoconid). The absence of a buccal cingulid and the presence of a distinctly broad trigonid basin, virtually at the same elevation as the talonid, make DAK-Arg-099 more similar to the lower molars of *Wadilemur*. For the DAK-Arg-099 lower molar, the configuration of the cristid obliqua (i.e., mesiolingually oriented and reaching the distal trigonid wall at a point between the protoconid and the metaconid) suggests us that this tooth is a M_2 rather than a M_1. In the latter case, we would expect the cristid obliqua to reach the trigonid wall at a point distal to the metaconid, as is often the case in the other stem

[1] *Karanisia* is documented by a highly crowned, styliform canine (Seiffert et al., 2003, fig. 1d, g), like that seen integrated and associated with similarly styliform incisors into the tooth-comb of crown strepsirrhines (i.e., tooth-combed Lorisiformes and Lemuriformes).

strepsirrhines such as djebelemurids and azibiids, and also several adapiforms (e.g., Adapids, Anchomomyines; e.g., Godinot, 2006; Marigó et al., 2011, 2013).

Concerning the DAK-Arg-103 upper molar, although this specimen is only half-preserved, it nevertheless provides characters that are primarily found in *Wadilemur*. These characters consist in the marked degree of angular invagination of the distal crown margin, demarcating the region of the distolingual cingulum, which appears as a protruding lobe bearing a small but well-defined hypocone. The distolingual lobe is not as distally extended as the condition observed on the upper molars of *Karanisia* (Seiffert et al., 2003; Jaeger et al., 2010), nor as buccolingually constricted and lingually displaced as on the single upper molar documenting *Saharagalago* (Seiffert et al., 2003), and is distinctly more developed than on the upper molars of *Djebelemur* (Marivaux et al., 2013) or *Omanodon* (Gheerbrant et al., 1993). The distal invagination of the crown is absent on upper molars of azibiids (*Azibius* and *Algeripithecus*; e.g., Tabuce et al., 2009). The condition in the latter is even the opposite, i.e., convex, and there is no distolingual lobe despite the presence of a prominent hypocone. The hypocone on DAK-Arg-103 is otherwise better developed, more cuspate than in *Karanisia* (tiny cusp) or in djebelemurids (absent in *Djebelemur*, virtually inexistent in *Omanodon*). The DAK-Arg-103 upper molar also differs from the upper molars of *Karanisia*, *Saharagalago*, and to a lesser extent those of djebelemurids, in the absence, as in *Wadilemur*, of the lingual cingulum, although this character cannot be properly assessed due to the partial preservation of the lingual flank of the protocone on the DAK C_2 specimen. On DAK-Arg-103, the development of a long and distobuccally oriented (oblique) postmetacrista is also found on upper molars of *Wadilemur*, but this character is particularly widespread, and especially well marked among several other early strepsirrhines from Afro-Arabia (notably *Djebelemur*, *Omanodon*, *Karanisia*, and *Saharagalago*, as well as caenopithecine adapids; e.g., Seiffert et al., 2018), except in azibiids and *Orolemur* (see below). The DAK-Arg-103 upper molar is almost the same size as the upper molars of *W. elegans*. The reconstruction of its missing parts (white lines; Fig. 6J) is modelled on the upper molars of *W. elegans* (Seiffert et al., 2005b, fig. 1A), and is therefore only tentative. It is worth noting that the preserved part matches particularly well the outline of the distal and lingual margins of *Wadilemur's* upper molars. However, DAK-Arg-103 differs in certain anatomical details, such as the presence of a very short, low prehypocrista (as also observed in *Saharagalago*), and the absence of a metaconule, which is vestigial (barely visible) in *W. elegans*. On DAK-Arg-103, the postprotocrista appears directly connected to the hypometacrista, whereas on upper molars of *W. elegans*, it seems that a hypometaconule crista (associated with the vestigial metaconule) links the postprotocrista to the hypometacrista. These subtle anatomical details may be present on the DAK-Arg-103, but the smoothed appearance of the occlusal surface makes them indistinguishable. Only better-preserved specimens would enable us to assess these features more accurately.

This upper molar fragment is compatible in size and occlusion with the DAK-Arg-099 lower molar, and both show strong affinities with molars of *W. elegans*. We therefore

consider these two isolated molars of DAK C_2 to represent the same taxon. However, given the paucity of the material and the subtle morphological differences noted, the formal attribution of these two specimens to *W. elegans* seems premature. We therefore prefer to refer these two teeth to *Wadilemur* cf. *elegans* at this stage. Adult body mass of this taxon from DAK C_2 is estimated at ~155 g on the basis of the area of the M_2 (DAK-Arg-099 area: 3.2 mm²; Table 1), calculated from the prosimian regression equation on M_2 provided by Egi et al. (2004). This diminutive extinct galagid primate from the Atlantic margin of Northwestern Africa was likely equivalent or slightly larger in size to the tiny living Zanzibar bush baby, *Galagoides zanzibaricus*, whose body mass varies between 137 and 150 g (after Harcourt and Bearder, 1989).

Infraorder ?Lorisiformes Gregory, 1915

Family indet.

Orogalago saintexuperyi gen. et sp. nov.

Etymology The genus name refers to the '*Rio de Oro*', the shallow and narrow inlet bounded by the Dakhla peninsula to the west and the African mainland coast to the east, with the Latin/translingual suffix *galago*, likely derived from the Wolof '*golo*', i.e., monkey. Epithet in honor of the renowned French aviator, writer, poet and reporter, Antoine de Saint-Exupery (1900–1944), pilot of the pioneering aviation company '*Aéropostale*', who landed on a regular basis at the '*Villa Cisneros*' (future city of Dakhla), a stopover on the famous airmail 'line'.

Holotype DAK-Arg-102, left M_2 (Fig. 7A–E).

Type locality Dakhla, El Argoub U4 level C_2 (DAK-Arg C_2), Atlantic margin of North-Saharan Africa (Fig. 1).

Formation and age Upper Samlat Formation, earliest Oligocene (earliest Rupelian; Benammi et al., 2019).

Diagnosis (based on the only known specimen, the holotype) Small taxon whose lower molar is characterized by a very short, extremely mesiodistally pinched trigonid, contrasting with a very long, broad talonid, also much lower in height; occlusal crown surface dominated by a projecting metaconid, relatively taller than the other three main cuspids (protoconid, hypoconid, and entoconid); absence of paraconid and hypoconulid; trigonid bordered mesially by a long, thin, very low, cingulid-like paracristid, directly connected to the base of the mesial flanks of the protoconid and metaconid, without any development of a mesially oriented buccal branch (preprotocristid) as in most other strepsirrhines; paracristid transversely oriented and parallel to the lateral and medial protocristids; presence of a strong buccal cingulid, limited to the hypoflexid and around the protoconid where it is particularly well developed, high and to some extent cuspidate (presence of a small accessory tubercle, directly buccal to the protoconid).

Nomenclatural remark This new genus and species must be referred to as *Orogalago saintexuperyi* Marivaux, 2024, following the article 50.1 and the "recommendation 50A concerning multiple authors" of the International Code of Zoological Nomenclature (ICZN, 1999).

Description Among the primate dental specimens collected at DAK C_2, one lower molar displays a somewhat unusual morphology, leading us to propose a new primate taxon. This single tooth has an almost square crown outline, being barely longer than it is wide (Fig. 7A), thereby suggesting that it is a second lower molar (M_2). Its main features are a very wide talonid and a particularly short trigonid (i.e., strongly pinched mesiodistally), virtually four times shorter than the talonid length. The occlusal structure comprises four main cuspids. The two buccal ones, protoconid and hypoconid, are pointed and slightly swollen at their base. In contrast, the two lingual ones, metaconid and entoconid, are sharper, buccolingually compressed and mesiodistally extended, appearing like dagger blades in buccal perspective (Fig. 7B). These two lingual cuspids are marginally situated, and their lingual aspect is particularly steep-sided. The trigonid basin is clearly higher than the talonid basin, and its metaconid is relatively taller than the other three main cuspids, projecting over the crown surface (Fig. 7B–E). The protoconid is slightly mesial to the metaconid on a buccolingual axis, and distinctly more lingual than the hypoconid on a mesiodistal axis (Fig. 7A), appearing to be positioned internally due to the presence of a strong buccal cingulid. The latter wraps around the protoconid and spans the hypoflexid, but disappears in front of the hypoconid (Fig. 7A–B). It is somewhat re-entrant at the level of the hypoflexid, thus generating a small invagination at the buccal base of the crown. This buccal cingulid is particularly well developed, high and to some extent cuspidate, directly buccal to the protoconid (presence of a small accessory tubercle; Fig. 7A–B, E). The protoconid and metaconid are connected by a long, thin, low and oblique (slightly distolingually oriented) protocristid, which consists of the union of a short branch corresponding to the lateral protocristid (stemming from the protoconid) with a longer branch corresponding to the medial protocristid (stemming from the metaconid) (Fig. 7A, D–E). Although the protocristid is not very elevated, it extends almost horizontally (slightly downward sloping) from the protoconid (i.e., lateral protocristid), then climbs steeply up the buccal flank of the tall metaconid (i.e., medial protocristid), thereby forming a wall that closes the trigonid distally (Fig. 7D–E). The medial protocristid extends up the buccal flank of the metaconid at its center, but does not reach the apex of the latter (stopping at the three-quarter slope). Mesially, the protoconid and metaconid are also connected by a long, thin and very low paracristid (i.e., cingulid-like cristid), much lower than the protocristid (Fig. 7A–C, E). This paracristid, connected to the base of the mesial flank of the protoconid, extends lingually (not mesially, i.e., absence of a mesially oriented buccal branch; the preprotocristid), horizontally (flat) and parallel to the protocristid, to reach the mesial base of the metaconid, thereby closing the trigonid mesially. The premetacristid is strong but extremely short, and not connected to the paracristid (i.e., it is not involved in mesiolingual closure of the trigonid). At the back of the crown, the vast talonid is walled all around its perimeter, resembling a large funnel (Fig. 7A–B, D). The hypoconid is distally canted and aligned with the entoconid

along a buccolingual axis. These two distal cuspids are connected by a strong, trenchant and very long hypocristid that extends distolingually (obliquely, backwards) in a straight line, merging in the distolingual crown margin region with the postentocristid, which is strong, relatively long and arched (Fig. 7A–B, D). The lingual talonid basin is also closed, but its wall is deeply indented (large V-shaped notch in buccal view; Fig. 7B). This deep incision in the lingual wall is related to the strong elevation of the metaconid and entoconid, and reflects the sloping deployment of the strong, short, steep postmetacristid, and the strong, long, gently sloping pre-entocristid, respectively. These lingual cristids also have a peculiar development, extending slightly inwards into the basin, so that the lingual wall/margin becomes invaginated (Fig. 7A). Buccally, the cristid obliqua is strong, long and sharp, with a deep, steep buccal side, and a gently sloping lingual side. From the hypoconid, the cristid obliqua extends mesiolingually, first plunging gently and then ascending in proximity to the trigonid (Fig. 7B). It runs up the distal trigonid wall and reaches its top at a point distolingual to the protoconid (closer to the protoconid than the metaconid), at the junction between the lateral and medial protocristids (Fig. 7B, D). Due to the configuration of the cristid obliqua, the hypoflexid is particularly well marked and deep (Fig. 7A–B).

Comparisons This single lower molar (DAK-Arg-102, M_2) is singular in its occlusal configuration, particularly with regard to its trigonid/talonid proportions (i.e., very short rectangular trigonid *versus* long, broad talonid), and the presence of some unusual morphological details in its occlusal pattern. These include the metaconid, which is much taller than the other three main cuspids and projects over the crown surface; the buccal cingulid, which is cusped directly buccal to the protoconid; and the lack a mesially oriented buccal branch of the paracristid (resulting in the marked mesiodistal compaction of the trigonid, appearing pinched mesiodistally). However, a broad talonid without hypoconulid, with a cristid obliqua extending mesiolingually to reach the distal trigonid wall at a point between the protoconid and the metaconid (generating a deep hypoflexid), and a compact trigonid slightly higher than the talonid, lacking the paraconid and with a very low, cingulid-like paracristid, is a suite of dental traits found primarily in strepsirrhines. There is no fossil taxon among known strepsirrhines whose lower molar morphology closely resembles the dental pattern of DAK-Arg-102. In addition to the prominent metaconid, another key differentiating feature of this tooth from molars of djebelemurids (*Djebelemur*, *'A.' milleri*, *Omanodon*, and *Shizarodon*), azibiids (*Azibius* and *Algeripithecus*) and known stem lorisiforms (*Karanisia*, *Saharagalago*, and *Wadilemur*) is the lack of a mesially oriented buccal branch of the paracristid (i.e., preprotocristid), which coincides with the compact buccal shape of the trigonid (i.e., short). A reduced mesial extension of the preprotocristid is, to a lesser extent, also observed in lower molars of *Plesiopithecus teras* from the latest Eocene of Egypt (Fayum L-41; Simons, 1992; Simons and Rasmussen, 1994). The latter is considered, together with *Propotto leakeyi* from the Early Miocene of Kenya (Simpson, 1967) as African stem chiromyiform lemurs that are exclusively related to the extant aye-aye, *Daubentonia*, from Madagascar (Gunnell et al., 2018). Although both taxa have lower molars with a surface-limited, short trigonid, and with a somewhat reduced mesial extension of the preprotocristid,

they do not show any projection of the metaconid as observed on DAK-Arg-102 (it is even the opposite in *Propotto*, where the metaconid is reduced and low), and instead show a stronger development of the paracristid, which is otherwise much obliquely oriented distolingually, as well as a cristid obliqua oriented mesiodistally and occupying a very buccal position, almost completely obstructing the hypoflexid (Gunnell et al., 2018: fig. 1). The latter feature particularly distinguishes DAK-Arg-102 from the lower molars of *Plesiopithecus* and *Propotto*. The DAK-Arg-102 M_2 further differs from lower molars of *Plesiopithecus*, in lacking a buccal cingulid wrapping around the base of the hypoconid, a character particularly marked in *Plesiopithecus*. In contrast, the DAK-Arg-102 rather shows a buccal cingulid spanning the hypoflexid and wrapping around the protoconid, in the latter case being strongly developed and high, appearing cuspidate, which results in the presence of a small accessory cuspid. A strong development of the buccal cingulid directly buccal to the protoconid is also observed on some *Propotto* specimens, but to a much lesser extent. Interestingly, a cuspidate buccal cingulid adjacent to the protoconid is not a feature exclusive to this taxon from DAK C_2. This peculiar and pronounced development is also observed in a living cheirogaleid lemuriforms, *Phaner furcifer* (e.g., Schwartz and Tattersall, 1985). Without forming a fully-fledged cuspid, a reinforcement of the buccal cingulid near the protoconid (likely enhancing occlusal and masticatory performance) is in fact widely distributed in extant strepsirrhines, including other species of cheirogaleids (e.g., *Mirza coquereli*), but also several species of lorisiforms, especially in certain galagids (e.g., *Euoticus elegantulus*, *Galagoides demidoff*; e.g., Schwartz and Tattersall, 1985), but also in some extant and extinct platyrrhine anthropoids (e.g., *Saimiri sciureus*, *Callithrix emiliae*, †*Neosaimiri fieldsi*, †*Antillothrix bernensis*, †'*Insulacebus*' *toussaintiana*, etc.; e.g., Takai, 1994; Cooke et al., 2011; Rosenberger et al., 2013).

A very short trigonid *versus* long, broad talonid, in addition to a very low, cingulid-like paracristid, with in several cases a very short development of the mesially oriented preprotocristid (i.e., buccal branch of the paracristid), a trenchant cristid obliqua extending mesiolingually and ending at a point lingual to the protoconid, and an entoconid displaying strong pre- and post- entoconid cristids are found in living cheirogaleid lemuriforms, but above all in living galagid and (some) lorisid lorisiforms, as well as in the extinct galagids such as the various species of *Komba* (see Harrison, 2010). It is for all these dental characteristics of lorisiforms found to a certain extent on DAK-Arg-102 that we favor affinities with this strepsirrhine group for this taxon from DAK C_2. However, validation of these proposed affinities will only be possible with the discovery of further fossils. Given the overall configuration of this primate lower molar (DAK-Arg-102) indicating affinities with strepsirrhines and possibly with lorisiforms, despite the severe lack of fossil material from DAK C_2, we nonetheless describe a new genus and species here due to the uniqueness of the morphological pattern of this single tooth: *Orogalago saintexuperyi* gen. et sp. nov. The adult body mass of this species is estimated at 290 g on the basis of the area of the DAK-Arg-102 M_2 (area: 4,9 mm^2; Table 1), by using the prosimian regression equation on M_2 provided by Egi et al. (2004). This diminutive extinct strepsirrhine from DAK C_2 was roughly equivalent in

size to the tiny living southern needle-clawed bush baby (*Euoticus elegantulus*) from western equatorial Africa, whose body mass varies between 271 and 300 g (after Kappeler, 1991).

Infraorder and Family indet.

Orolemur mermozi gen. et sp. nov.

Etymology The genus name refers to the '*Rio de Oro*', the shallow and narrow inlet bounded by the Dakhla peninsula to the west and the African mainland coast to the east, with the suffix *lemur* from the Latin *lemures*, i.e., spirits of the dead. Epithet in honor of the renowned French aviator Jean Mermoz (1901–1936), pilot of the pioneering aviation company '*Aéropostale*', who landed on a regular basis at the '*Villa Cisneros*' (future city of Dakhla), a stopover on the famous airmail route.

Holotype DAK-Pto-055, a virtually pristine right M^1 or M^2 (Fig. 7F–J).

Type locality Dakhla, Porto Rico U4 level C_2 (DAK-Pto C_2), Atlantic margin of North-Saharan Africa (Fig. 1).

Formation and age Upper Samlat Formation, earliest Oligocene (earliest Rupelian; Benammi et al., 2019).

Diagnosis Diminutive strepsirrhine taxon with triangular occlusal outline of upper molar(s), characterized by a large trigon basin resulting from widely spaced but equidistant positions of the paracone, metacone and protocone (absence of hypocone); presence of complete, well-marked and fairly strong buccal and lingual cingula, and short mesial and distal cingula, the distal one being limited to the midline of the crown rather than extending buccally; presence of tiny, barely visible conules, with a unusually long postmetaconule crista extending buccodistally (i.e., occupying the place where the buccal part of the distal cingulum would normally be); absence of parastyle and metastyle, as well as absence of buccal development of the postmetacrista (no metastylar shelf).

Nomenclatural remark This new genus and species must be referred to as *Orolemur mermozi* Marivaux, 2024, following the ICZN (1999:Art. 50.1).

Description The DAK-Pto-055 upper molar (M^1 or M^2, the holotype; Fig. 7F–J) is virtually pristine. It has a triangular crown outline, with a slightly invaginated distal margin. Its occlusal structure is simple, consisting of three main, salient cusps, appearing somewhat internally positioned due to the development of strong buccal and lingual cingula. The paracone dominates the two other main cusps (metacone and protocone), being taller and particularly pointed (Fig. 7G–I). The metacone is situated far distally to the paracone, but aligned with the latter along a mesiodistal axis. Both cusps are linked by long, trenchant postparacrista and premetacrista. The latter are slightly inclined and close the trigon basin buccally, giving it a wide V-shaped indentation in lingual (Fig. 7G) and buccal (Fig. 7H) perspectives. The

postparacrista is longer due to the greater elevation of the paracone. The preparacrista and postmetacrista are present but less developed, appearing as very short, steeply sloping crests. The pre- and post- paracone and metacone cristae are aligned along a mesiodistal axis. A well-defined, continuous buccal cingulum extends mesiodistally from the mesial end of the preparacrista to the distal end of the postmetacrista. It forms a full-fledged enamel shelf, buccal to the paracone and metacone (Fig. 7F, H–J). In its center, between the paracone and metacone, but not aligned with them, located on the buccal margin, this cingulum bears a mesiodistally extended enamel swelling, corresponding to a mesostyle. Lingually, the protocone is practically equidistant from the two buccal cusps, so that the apices of the three cusps form an equilateral triangle (Fig. 7F). The protocone displays two strong crests nearly equal in length, and almost symmetrical in configuration, one directed mesiobuccally, the preprotocrista, and the other distobuccally, the postprotocrista. These two crests give the protocone a very flared U-shape. The lingual flank of the protocone (plus its pre- and post-cristae) is steep, whereas its buccal flank slopes gently into the trigon basin. The buccal flank of the protocone forms a sort of pillar oriented buccolingually (i.e., endoprotocrista), appearing as a distinct relief on the lingual aspect of the trigon basin (Fig. 7F, H). On the midline of the crown, two small enamel swellings can be seen, flanked on the mesial and distal margins. The mesial one is identified as a tiny paraconule, while the distal one (barely visible and displaced very distally) is identified as a tiny metaconule. The paraconule is connected lingually to the preprotocrista. Mesiobuccally, it displays a very low preparaconule crista that extends to the base of the mesial end of the preparacrista, just at the beginning of the buccal cingulum (Fig. 7F–G, J). Distally, the metaconule displays a well-defined, long, thin and oblique hypometaconule crista, which connects to the buccal end of the postprotocrista (Fig. 7F–G, I). Distobuccally, it displays a thin postmetaconule crista that extends to the base of the distal end of the postmetacrista, just at the beginning of the buccal cingulum (Fig. 7F–G, I–J, D). The preparaconule crista and ‘postmetaconule crista plus hypometaconule crista’ complex have the same direction as the preprotocrista and postprotocrista, respectively, which make the trigon basin very long and ample (a very flared U-shape). Furthermore, there is no trace of hypoparacrista and hypometacrista development on the lingual flanks of the paracone and metacone, respectively, which remain free-standing and steep-sided, thereby making the trigon basin (unobstructed) particularly extensive. The protocone, as with the paracone and metacone, appears internally positioned due to the development of a strong, almost continuous lingual cingulum. There is a small, shallow indentation in its distolingual region that superficially punctuates its continuity (Fig. 7G, I). This lingual cingulum runs at the base of the crown, starting at a point directly mesiolingual to the paraconule (i.e., short mesial cingulum; Fig. 7F–G, J), and ending distally, at a point directly distal to the metaconule (i.e., short distal cingulum; Fig. 7F, I). There is no hypocone, only a minuscule enamel protuberance occurs in the distolingual region of the cingulum, which may result from the shallow indentation described above (Fig. 7F–G, I). In contrast, there is a minute enamel swelling, located directly lingual to the protocone, which could correspond to a small pericone (Fig. 7F–G, I–J).

Comparisons The occlusal pattern of the DAK-Pto-055 upper molar (M^1 or M^2) is singular and somewhat unique among primates known from the Paleogene of Afro-Arabia. A triangular crown outline (accentuated by a pronounced spacing between the paracone and metacone), the lack of both hypoparacrista and hypometacrista, the absence of hypocone, the presence of a sub-continuous but strong lingual cingulum, and the development of a well-marked and mesiodistally stretched mesostyle, are dental traits whose association can be found, to some extent, in early strepsirrhines. Compared with strepsirrhines of Afro-Arabia, DAK-Pto-055 differs from upper molars of djebelemurids, such as *Djebelemur* and *Omanodon* (the upper dentition of '*A*.' *milleri* and *Shizarodon* being so far unknown; Simons, 1997; Gheerbrant et al., 1993; Marivaux et al., 2013), in displaying a sub-continuous lingual cingulum and a strong, complete, full-fledged buccal cingulum bearing a well-defined mesostyle in its center, in the absence of parastyle and metastyle, in the lack of a long postmetacrista development in the distobuccal region of the crown (no metastylar shelf), and above all, in showing the presence of a postmetaconule crista, which runs from a tiny metaconule towards the distobuccal corner of the tooth. The latter crest occupies/replaces the buccal part of the distal cingulum, which is much shorter as a result (limited in its lingual part). The DAK-Pto-055 upper molar also differs substantially from upper molars of *Karanisia* (Seiffert et al., 2003; Jaeger et al., 2010), as it lacks the extensive distolingual development of the lingual cingulum, which forms a full-fledged talon lobe bearing a minute hypocone in this taxon. The same is true for *Saharagalago* and *Wadilemur* (Seiffert et al., 2003, 2005b), which show upper molars with, in addition, a strongly waisted distal crown margin, bearing a well-defined, cuspate hypocone developed on the distolingual cingulum, as well as the presence of a parastyle on the buccomesial corner of the crowns, less conspicuous buccal cingulum development, and the lack of postmetaconule crista. The DAK-Pto-055 upper molar also differs from upper molars of azibiids, *Algeripithecus* and *Azibius* (e.g., Tabuce et al., 2009) in being much less bunodont, in lacking the conspicuous hypocone, in having a buccal cingulum better marked (including a mesostyle), a shorter distal cingulum, and in displaying a long postmetaconule crista distobuccally directed. It also differs from *Plesiopithecus* (Simons, 1992; Simons and Rasmussen, 1994; Gunnell et al., 2018) in developing a postmetaconule crista, in having a shorter distal cingulum, and in displaying a stronger buccal cingulum bearing a mesostyle. On the DAK-Pto-055 upper molar, the presence of a strong and full-fledged buccal cingulum bearing a mesostyle, the development of trenchant buccal shearing crests, especially the postparacrista and premetacrista, the lack of hypoparacrista and hypometacrista, and the presence of prominent mesial and lingual cingula, are dental traits characterizing upper molars of the caenopithecine adapids, primarily documented in the late Eocene of Egypt (Fayum; Simons et al., 1995; Simons and Miller, 1997; Godinot, 1998; Seiffert et al., 2009, 2018). However, the upper molars of these large-bodied adapids have a more quadrangular crown outline without any invagination of their distal margin, display a conspicuous hypocone, a stronger and longer shearing eocrista (W-shaped) with well-developed preparacrista and postmetacrista, and do not show any development of the postmetaconule crista, which is prominent on DAK-Pto-055. The development of a postmetaconule crista is

unique among stem strepsirrhines from Afro-Arabia, in which there is no development of the latter character, nor of a metaconule in most cases. A minute, vestigial metaconule can be observed in azibiids (Godinot and Mahboubi, 1992, 1994; Tabuce et al., 2009), in *Wadilemur elegans* (Seiffert et al., 2005b), and in caenopithecine adapids (Simons et al., 1995; Simons and Miller, 1997; Seiffert et al., 2009, 2018; with the exception of *Notnamaia*, where the metaconule is cuspate and clearly visible; Godinot et al., 2018). A long postmetaconule crista extending distobuccally, although unusual is also observed, likely developed convergently, in certain sivaladapid adapiforms from the Oligocene and Miocene of South Asia (e.g., *Guangxilemur* and *Sivaladapis*; Gingerich and Sahni, 1984; Qi and Beard, 1998; Marivaux et al., 2002), but also strikingly in a Miocene tarsiid tarsiiform from South East Asia (*Tarsius sirindhornae*; Chaimanee et al., 2011), and in some afrotarsiid eosimiiforms from the Paleogene of South Asia and North Africa (*Afrasia* and *Afrotarsius*; Jaeger et al., 2010; Chaimanee et al., 2012). This DAK-Pto-055 upper molar is incompatible in size and morphology to be associated with the DAK-Pto-054 lower molar described above and referred to as *Afrotarsius* sp. In addition, DAK-Pto-055 lacks the most diagnostic afrotarsiid dental characters. Indeed, although this upper molar displays a well-marked buccal cingulum, the latter is not as extensive as in afrotarsiids. It also lacks a long, arched postmetacrista and a metastyle (strong and displaced buccally, forming a metastylar shelf), as well as the hypometacrista and hypoparacrista, as seen on upper molars of *Afrasia* and *Afrotarsius*.

To some extent, the morphology of the DAK-Pto-055 upper molar, could better match that of some anchomomyin notharctids from the Eocene of Europe (e.g., *Anchomomys gaillardi*, *Anchomomys frontanyensis*, *Nievesia sossisensis*; e.g., Marigó et al., 2011, 2013). However, DAK-Pto-055 has a more complete lingual cingulum, no sign of 'incipient' hypocone, displays a stronger buccal cingulum without parastyle and metastyle (no metastylar shelf), has no hypometacrista, and displays a short distal cingulum that does not extend buccally. In contrast, it exhibits a strong and long postmetaconule crista (absent in anchomomyins) extending distobuccally, and thus occupying the place of the buccal part of the distal cingulum (the latter being complete, extending buccally in anchomomyins).

During the review process of the manuscript of this article, two of the three reviewers suggested that the DAK-Pto-055 upper molar might be associated with the DAK-Arg-102 lower molar (Fig. 7A–E), which designates the holotype of *Orogalago saintexuperyi* (see above). However, given the absence of a hypocone on the DAK-Pto-055 upper molar (Fig. 7F), one might expect the morphology of the probable lower molar to compensate for optimal occlusion and function, through the presence of a long, broad trigonid bearing a remarkably large paraconid (or another large mesially located cuspid). This is not the case with the DAK-Arg-102 lower molar, which presents a reduced, very short, mesiodistally pinched trigonid, with no paraconid or compatible other cuspid. The trigonid structure of DAK-Arg-102 lower molar seems to us incompatible with the morphology of the DAK-Pto-055 upper molar in terms of functional efficiency in occlusion. However, the DAK-Arg-102 lower molar displays an extensive distolingual crown area resulting from the strong development of the

postentocristid and the long buccolingually extended hypocristid. This distolingual complex could possibly compensate for the brevity of the trigonid on the following lower molar, and could, to some extent, be more functional with the absence of a hypocone on the upper molars. Nevertheless, in terms of size compatibility, the DAK-Pto-055 upper molar appears to be too small to match the size of the DAK-Arg-102 lower molar (see also the incompatibility of estimated body masses; Table 1). In the absence of more comprehensive dental material, and given the size and certain occlusal incompatibilities of these two teeth, we suggest that these two specimens represent two distinct taxa. We then propose here a new taxon, *Orolemur mermozi* gen. et sp. nov., illustrating the unusual and somewhat unique morphology of the DAK-Pto-055 upper molar. Adult body mass of this new taxon is estimated at 160–163 g on the basis of the upper molar area (DAK-Pto-055 area: 5.0 mm^2; Table 1), by using the prosimian regression equations (M^1 and M^2) provided by Egi et al. (2004). This diminutive extinct strepsirrhine primate from the Atlantic margin of Northwestern Africa was likely equivalent in size to the tiny living Malagasy cheirogaleid lemur, *Cheirogaleus medius*, whose body mass varies between 142 and 217 g (after Mittermeier et al., 1994). It was also about the same size as the extinct galagid *Wadilemur elegans*.

4. Discussion and conclusions

Based on fossil dental remains, this earliest Oligocene primate community from Dakhla (DAK C_2 level; ca. 33.5 Ma) reported here provides a unique glimpse into the paleodiversity of anthropoids and strepsirrhines at that time on Africa's northwestern margin (nowadays the Atlantic margin of the Sahara). The same is true for rodents (anomaluroids and hystricognaths) found in the same fossil-bearing level (Marivaux et al., 2017a, b). Nevertheless, this seemingly great diversity is not illustrated by a large number of dental specimens (22 teeth of primates), despite the large amount of sediment processed to date (~5 tons). Some identifications are based on a single isolated tooth, or even a tooth fragment. It is therefore highly likely that only a fraction of the total paleodiversity of the primate community of this Atlantic coastal region of northwestern Africa has been so far documented. Primates and rodents of the late Eocene–early Oligocene time interval have hitherto only been documented by fossil assemblages from northern and northeastern Africa (eastern Algeria, central Libya, and northern Egypt), eastern Sub-Saharan Africa (Kenya), and southeastern Arabia (Dhofar in Oman). The primate and rodent data from Dakhla are therefore particularly important as they provide new insights into the paleogeography of these mammals near the Eocene/Oligocene transition (EOT; ca. 34 Ma). The presence of anthropoid and strepsirrhine primates a well as hystricognathous rodents in DAK C_2 is not unexpected because these mammal groups (in addition to afrotherian taxa) were among the most common members of Afro-Arabian mammal faunas known during the late Eocene–early Oligocene time interval. However, the presence of diversified anomaluroid rodents in DAK C_2

is unequaled at the Afro-Arabian scale[2] for the early Oligocene epoch (Marivaux et al., 2017b). If the anomaluroids provide a unique taxonomic record of that rodent group, most of the hystricognaths, anthropoids and strepsirrhines from the same DAK C_2 level, primarily document close relatives of taxa known from the famous Egyptian fossil-bearing localities of the Jebel Qatrani Formation (Fayum Depression; see Seiffert, 2006, 2012), dating either from the latest Eocene (most taxa) or the early Oligocene (a few other taxa) (Fig. 8). In Dakhla, we record the occurrence of at least eight primate species documenting distinct families. Four of them are among the Anthropoidea, including an oligopithecid (*Catopithecus* aff. *browni*), a parapithecid (*Abuqatrania* cf. *basiodontos*), a propliopithecid (?*Propliopithecus* sp.), and an afrotarsiid (*Afrotarsius* sp.). Four other species belong to the Strepsirrhini, including a djebelemurid (cf. '*Anchomomys*' *milleri*) and a galagid (*Wadilemur* cf. *elegans*), as well as two new forms among which a possible lorisiform (*Orogalago saintexuperyi* gen. et sp. nov.) and a strepsirrhine of indeterminate affinities (*Orolemur mermozi* gen. et sp. nov.). Four of these primates, such as the oligopithecid, parapithecid, djebelemurid and galagid are known (at least in very similar forms) from the latest Eocene site L-41 in Egypt (Fayum) (Fig. 8). The presence of a parapithecid on the Atlantic margin of North Africa is not surprising, as this group of primates was widespread during the Paleogene, known in northern and northeastern Africa, in southeastern Arabia, as well as in eastern sub-Saharan Africa (for a summary, see Ducrocq et al., 2011; Seiffert, 2012), and even in South America during the early Oligocene (Peruvian Amazonia, *Ucayalipithecus*, a *Qatrania*[3]-like taxon; Seiffert et al., 2020). If the arrival of the Parapithecidae in South America is thought to be the result of rafting from Africa (Seiffert et al., 2020), parapithecids were obviously present along the West African coast. The same applies to the Oligopithecidae, if it turns out that this African primate group was also represented in South America during the early Oligocene (Peruvian Amazonia, *Perupithecus*, a *Talahpithecus*[4]-like taxon; Bond et al., 2015; Marivaux et al., 2023). We can extend this reasoning to hystricognathous rodents (e.g., Antoine et al., 2012; Marivaux and Boivin, 2019). Primates and rodents in Africa certainly had a more widespread geographic distribution than that indicated by the limited locations of their few known fossils, and they probably lived in other regions for which we have no records. This new fossil record from Dakhla provides compelling evidence for a broader geographic distribution of these mammals, at least across North Africa, during the late Eocene–earliest Oligocene.

A noteworthy finding is the presence of a small propliopithecid primate in the earliest Oligocene of Dakhla. Despite its very fragmentary nature, limited to a portion of talonid of a lower molar (Fig. 3Q–S), this unique fossil testifies to the oldest occurrence of this anthropoid family in Africa, since its counterparts are well documented in Egypt and Oman, but in sites that are 2–3 Ma younger on the early Oligocene biostratigraphic scale (see Seiffert, 2006,

[2] An anomalurid anomaluroid is also reported from lower Oligocene deposits in Oman (Thomas et al., 1992), but it has not been described to date. A zenkerellid anomaluroid has also been described from central Libya (Coster et al., 2015), with a diminutive *Zenkerella*-like taxon from lower Oligocene deposits of the Zallah Oasis (*Prozenkerella saharaensis*).

[3] *Qatrania* is a parapithecid from the early Oligocene of Egypt (Fayum; e.g., Simons and Kay, 1983).

[4] *Talahpithecus* is an oligopithecid from the late Eocene of Libya (Dur At-Talah; Jaeger et al., 2010).

2007a, 2012) (Fig. 8). Although the sister group of propliopithecids and later catarrhines probably consists of oligopithecids (e.g., Simons and Rasmussen, 1996; Seiffert and Simons, 2001; Seiffert, 2012) known as early as the late Eocene in the Fayum (L-41) and Dur At-Talah (Libya; Jaeger et al., 2010), large-bodied propliopithecids (i.e., *Propliopithecus*, *Aegyptopithecus*, and *Moeripithecus*) appear as such somewhat suddenly in the early Oligocene fossil record of the Fayum in Egypt (quarries G/V and I/M, upper sequence of Jebel Qatrani Formation; Fig. 8). The lack of knowledge about primitive catarrhines whose morphology would be intermediate between oligopithecids and propliopithecids is perhaps simply due to gaps in sampling and/or sedimentation in Northeast Africa (Seiffert, 2006). However, the fossil record from Afro-Arabia documenting the latest Eocene–earliest Oligocene interval (especially the earliest Oligocene) is so poorly known that it is possible that pre-propliopithecids (the purported 'transitional' forms) could have originated in another region of Afro-Arabia. Despite its very fragmentary nature, this somewhat less bunodont and medium-sized taxon from Dakhla could be a potential candidate for documenting a representative of these purported intermediate forms. However, more nearly complete specimens of this taxon will be required to test this possibility. Absent from the latest Eocene record of the Fayum (L-41), their presence in the earliest Oligocene of Dakhla (fossil record close to that of L-41), could also suggest that these primates may have occupied a special ecological niche in northwestern Africa, which was apparently not available or already occupied in Northeast Africa at that time. Indeed, in Dakhla, we so far do not record any trace of the large-bodied anthropoid-like caenopithecine adapids (Adapiformes), well documented in the Fayum during the late Eocene (Simons et al., 1995; Simons and Miller, 1997; Godinot, 1998; Seiffert et al., 2009, 2018; Seiffert, 2012). Large-bodied propliopithecids appear in the Oligocene fossil record of the Fayum while large-bodied adapids are no longer recorded (Fig. 8). In Oman, propliopithecids are recorded together with oligopithecids, but no trace of caenopithecine adapids has hitherto been mentioned (Thomas et al., 1988, 1991; Gheerbrant et al., 1993, 1995). Considering our new observation from Dakhla and on the basis of the rich documentation from the Fayum over time and from Oman, the occurrence and distribution of propliopithecids *versus* caenopithecine adapids could reflect a case of ecological exclusion of both large-bodied primate groups in Afro-Arabia at that time. However, given the incompleteness of the primate record from DAK C_2, it cannot be ruled out that future discoveries at this site will yield caenopithecines, in which case this hypothesis of exclusion would be invalidated.

With such a high diversity of primates and rodents recorded in DAK C_2, especially the presence of various anomaluroids assumed to live in densely forested environments (see Marivaux et al., 2017b; Fabre et al., 2018), it can be expected that during the earliest Oligocene, paleoenvironmental conditions at this tropical latitude were particularly favorable, with likely coastal forests fringing the western (Atlantic) margin of North Africa. The temporal proximity and faunal resemblance (primate and hystricognath assemblages) between DAK C_2 in the west and L-41 in the east (Fig. 8), reveal a widespread east-west distribution of several mammals, thereby underscoring, to some extent, similar tropical environmental conditions in

northern latitudes of Africa during the latest Eocene–earliest Oligocene time interval. The extensive east-west geographic distance was likely characterized by difference in habitats, which was otherwise the likely source of alpha-level diversity among early Afro-Arabian primates and rodents (and probably other mammals). However, the taxonomic proximity between L-41 (Fayum) and DAK C_2 (Dakhla) at the generic level (even specific) suggests the existence of an east-west 'trans-North African' forested environmental continuum during the latest Eocene–earliest Oligocene time interval (Marivaux et al., 2017a), or at least that there was no fundamental barrier to free dispersal between the Atlantic margin of North Africa and northern Egypt at that time. However, local differences in paleoenvironmental conditions, particularly in forest structures, as well as ecological competitions, most certainly played a selective role in the presence or absence of certain mammal groups or genera, resulting in apparent faunal distinctions between the northwestern and northeastern provinces of Afro-Arabia (e.g., presence of anomaluroid rodents at DAK C_2 *versus* absence at L-41, whereas they were present earlier in time at BQ-2 in the same Fayum region; absence of proteopithecid anthropoids and adapid adapiforms at DAK C_2, whereas they were common at L-41; presence of singular strepsirrhines at DAK C_2, nowhere else known). The absence of certain groups of mammals at Dakhla is not necessarily a real absence, but may be related to taphonomic reasons, either because these mammals were very rare, or because they lived in areas different or distant from the environment in which the DAK C_2 fossil-bearing level was deposited. Renewed field efforts and further wet screening of the DAK C_2 sediments should provide more fossils in the future, and then a more comprehensive list of mammals that lived in the area at that time.

The mammal assemblage from the earliest Oligocene of Dakhla shows that primates (anthropoids and strepsirrhines) and rodents (hystricognaths and anomaluroids) were particularly diversified, both taxonomically and ecologically (wide range of body-sizes), at the time of the drastic global climate change characterizing the Eocene/Oligocene transition (EOT; e.g., Zachos et al., 2008; Bohaty et al., 2012; Tramoy et al., 2016; Westerhold et al., 2020). The latter marked the shift from 'greenhouse' Eocene conditions to 'icehouse' conditions at the beginning of the early Oligocene and beyond, and was associated to faunal turnovers and ecological restructuring in many parts of the world, as particularly documented in the Holarctic Province (e.g., Stehlin, 1909; Savage and Russell, 1983; Janis, 1993; Berggren and Prothero, 1992; Meng and McKenna, 1998; Coxall and Pearson, 2007; Zanazzi et al., 2007; Weppe et al., 2023). This global climatic event was dramatic for primate communities, leading to their extirpation across the whole of the Holarctic continents, with the exception of regions that extended into lower latitudes, allowing continuous access to tropical refugia (e.g., Gingerich and Sahni, 1984; Beard, 1998a, b; Qi & Beard, 1998; Köhler and Moyà-Solà, 1999; Marivaux et al., 2001, 2002, 2005, 2006, 2023; Jablonski, 2003, 2005; Marivaux, 2006; Bond et al., 2015; Seiffert, 2007a, b, 2012; Ni et al., 2016; Seiffert et al., 2020; Rust et al., 2023). There was so far no fossil-bearing locality in Africa dating from the earliest Oligocene (ca. 33.5 Ma). The fossil record of DAK C_2 is therefore the only faunal reference on that landmass, occurring at the very early stage of global climatic deterioration (Fig. 8). The highly

diverse mammal record of DAK C_2 (including arboreal thermophilic species such as the strepsirrhines and anomaluroids) suggests that this tropical region of Northwest Africa was apparently less affected, if at all, by the cooling and associated paleoenvironmental changes recorded at that time, or at least that the effects were delayed. The expected densely forested paleoenvironment that was fringing the western margin of North Africa is likely to have offered better temperate or even tropical refugia than higher latitudes or areas further inland during the cooling event. The environmental degradation, by fostering the fragmentation of forest habitats, may have been much more gradual in low latitudes, such as tropical North Africa, than in high latitudes (i.e., Holarctic Province) where paleoenvironmental changes were more abrupt and associated with a profound reorganization of ecosystems. Fossil-bearing localities of North Africa that are 2–3 Ma younger than DAK C_2 (Fig. 8; e.g., upper sequence of the Jebel Qatrani Formation in Fayum, northeastern Egypt, or Zallah Oasis, central Libya) have quite distinct faunal compositions, without any strepsirrhine (e.g., Rasmussen et al., 1992; Gagnon, 1997; Seiffert, 2007a, 2012; Beard et al., 2016, 2017; de Vries et al., 2021; Mattingly et al., 2021). They also reflect a certain degree of endemism (faunal provincialism), probably the result of habitat fragmentation having generated some kind of geographical barriers to dispersal, which in turn favored allopatric speciation among previously widespread populations (e.g., Beard et al., 2016, 2017; Mattingly et al., 2021). The subsequent/delayed environmental changes likely constricted the latitudinal range of arboreal strepsirrhines and anomaluroids in equatorial Africa, and might have driven into extinction some other lineages in North Africa (e.g., adapids, djebelemurids, anomalurids, etc.). The fossil record of Taqah in Oman (early Oligocene, ca. 31 Ma), including strepsirrhines, anthropoids, hystricognaths, anomalurids, cricetids and afrotheres (Thomas et al., 1992), illustrates warm, forested and favorable environmental conditions that bordered the southern margin of the Arabian Peninsula. These exceptional marginal conditions that prevailed a few million years beyond the EOT in Oman may have resulted in the local survival (a temporary reprieve) of strepsirrhines and anomalurids, otherwise extirpated in Northeast Africa at the same time (Seiffert, 2007a; 2012; Beard et al., 2017).

Further fieldwork in the Dakhla region of the Sahara, in search for mammal-bearing deposits from the latest Eocene but more particularly from younger levels of the early Oligocene, would provide a better view of these envisaged 'delayed' effects, at least locally, linked to the EOT climate and environmental changes in the Atlantic margin of North Africa. This would make it possible to document patterns of extinction or diversification that may have occurred as a result of habitat fragmentation linked to the global climatic deterioration, or increased seasonality in this tropical low latitude of Africa.

Acknowledgments

We are particularly indebted to Henri Cappetta† (ISE-M, France), Sébastien Enault (ISE-M, *Kraniata*, France) and Jérôme Surault (PALEVOPRIM, France), as well as Imad Elkati, Abdallah

Tarmidi and Mbarek Fouadasi (Morocco), and the local people of Dakhla for their assistance during the successive field seasons (2009–2023). Many thanks to Gérard Barbe (France) and Benjamin D'Haeze (Belgium) for their interest in our paleontological project in the Dakhla region. We are grateful to Sandra Unal, Suzanne Jiquel and Bernard Marandat (ISE-M), Théo Mancuso (*Université de Montpellier*, France), and Jérôme Surault (PALEVOPRIM) for their contribution in the picking of the fossil specimens from Porto Rico and El Argoub. We gratefully acknowledge Narla S. Stutz (ISE-M) for her advice on zoological nomenclature. We would like to thank Chris Beard (The University of Kansas, Lawrence, USA) and the two other anonymous reviewers, as well as Mark Grabowski (co-Editor-in-chief, JHE) and Raef Minwer-Barakat (Associate Editor, JHE) for their comments, remarks and expert suggestions, which substantially enhanced the final version of the manuscript. 3D renderings of digital models of fossil specimens were obtained using the µCT-scanning facilities (ISE-M, Montpellier, France) of the Montpellier RIO Imaging (MRI), supported by the LabEx CeMEB. This research received financial support from the French programs ANR-ERC PALASIAFRICA (ANR-08-JCJC-0017) and ANR EVAH (ANR-09-BLAN-0238), the MEDYNA program (FP7, PIRSES-GA-2013-612572), the CNRS-CoopIntEER program (171834), and from the ISE-M UMR 5554 (*Laboratoire de Paléontologie*) and PALEVOPRIM UMR 7262. This is ISE-M publication 2024-104 SUD.

References

Adnet, S., Cappetta, H., Enault, S., Benammi, M., Marivaux, L., Tabuce, R., Saddiqi, O., Baidder, L., Benammi, M., 2017. The late Eocene/Oligocene elasmobranch fauna of the Samlat Formation in Dakhla, Morocco: a mirror of the coeval World Heritage sites of Egypt. The First West African Craton and Margins International Workshop (WACMA1), April 24-29th, 2017, Dakhla, Morocco, pp. 81–82.

Antoine, P.-O., Marivaux, L., Croft, D.A., Billet, G., Ganerød, M., Jaramillo, C., Martin, T., Orliac, M.J., Tejada, J., Altamirano, A.J., Duranthon, F., Fanjat, G., Rousse, S., Salas-Gismondi, R., 2012. Middle Eocene rodents from Peruvian Amazonia reveal the pattern and timing of caviomorph origins and biogeography. Proc. Roy. Soc. B 279, 1319–1326.

Beard, K.C., 1998a. East of Eden: Asia as an important center of taxonomic origination in Mammalian evolution. In: Beard, K.C., Dawson, M.R. (Eds.), Dawn of the Age of Mammals in Asia. Bull. Carnegie Mus. Nat. Hist., pp. 5–39.

Beard, K.C., 1998b. A new genus of Tarsiidae (Mammalia: Primates) from the middle Eocene of Shanxi Province, China, with notes on the historical biogeography of tarsiers. In: Beard, K.C., Dawson, M.R. (Eds.), Dawn of the Age of Mammals in Asia. Bull. Carnegie Mus. Nat. Hist., pp. 260–277.

Beard, K.C., 2002. Basal anthropoids. In: Hartwig, W.C. (Ed.), The Primate Fossil Record. Cambridge University Press, Cambridge, pp. 133–149.

Beard, K.C., 2004. The Hunt for the Dawn Monkey. Unearthing the Origins of Monkeys, Apes, and Humans. University of California Press, Berkeley.

Beard, K.C., 2013. Anthropoid origins. In: Begun, D.R. (Ed.), A Companion to Paleoanthropology. Wiley Online Books, pp. 358–375.

Beard, K.C., Coster, P.M.C., 2016. Brief communication: Upper molar morphology of the early Oligocene Egyptian anthropoid *Qatrania wingi*. Am. J. Phys. Anthropol. 159, 714–721.

Beard, K.C., Coster, P.M.C., Salem, M.J., Chaimanee, Y., Jaeger, J.-J., 2016. A new species of *Apidium* (Anthropoidea, Parapithecidae) from the Sirt Basin, central Libya: First record of Oligocene primates from Libya. J. Hum. Evol. 90, 29–37.

Beard, K.C., Coster, P.M.C., Salem, M.J., Chaimanee, Y., Jaeger, J.-J., 2017. Biogeographic provincialism shown by Afro-Arabian mammals during the middle Cenozoic: climate change, Red Sea rifting and global eustasy. In: Agius, D.A., Khalil, E., Scerri, E.M.L., Williams, A. (Eds.), Human Interaction with the Environment in the Red Sea - Selected Papers of Red Sea Project VI. Koninklijke Brill NV, Leiden, pp. 48–68.

Benammi, M., Adnet, S., Marivaux, L., Yans, J., Noiret, C., Tabuce, R., Surault, J., El Kati, I., Enault, S., Baidder, L., Saddiqi, O., Benammi, M., 2019. Geology, biostratigraphy and carbon isotope chemostratigraphy of the Paleogene fossil-bearing Dakhla sections, Southwestern Moroccan Sahara. Geol. Mag. 156, 117–132.

Berggren, W.A., Prothero, D.R. (Eds.), 1992. Eocene-Oligocene Climatic and Biotic Evolution: an Overview. Princeton University Press, Princeton.

Bohaty, S.M., Zachos, J.C., Delaney, M.L., 2012. Foraminiferal Mg/Ca evidence for Southern Ocean cooling across the Eocene–Oligocene transition. Earth Planet. Sc. Lett. 317–318, 251–261.

Bond, M., Tejedor, M.F., Campbell Jr, K.E., Chornogubsky, L., Novo, N., Goin, F.J., 2015. Eocene primates of South America and the African origins of New World monkeys. Nature 520, 538–541.

Chaimanee, Y., Lebrun, R., Yamee, C., Jaeger, J.-J., 2011. A new Middle Miocene tarsier from Thailand and the reconstruction of its orbital morphology using a geometric-morphometric method. Proc. Roy. Soc. B 278, 1956–1963.

Chaimanee, Y., Chavasseau, O., Beard, K.C., Kyaw, A.A., Soe, A.N., Sein, C., Lazzari, V., Marivaux, L., Marandat, B., Swe, M., Rugbumrung, M., Lwin, T., Valentin, X., Thein, Z.M.M., Jaeger, J.-J., 2012. A new middle Eocene primate from Myanmar and the initial anthropoid colonization of Africa. Proc. Natl. Acad. Sci. USA 109, 10293–10297.

Cooke, S.B., Rosenberger, A.L., Turvey, S., 2011. An extinct monkey from Haiti and the origins of the Greater Antillean primates. Proc. Natl. Acad. Sci. USA 108, 2699–2704.

Coster, P.M.C., Beard, K.C., Salem, M.J., Chaimanee, Y., Jaeger, J.-J., 2015. New fossils from the Paleogene of central Libya illuminate the evolutionary history of endemic African anomaluroid rodents. Front. Earth Sci. 3, 56.

Court, N., 1993. An enigmatic new mammal from the Eocene of North Africa. J. Vert. Paleontol. 13, 267–269.

Coxall, H.K., Pearson, P.N., 2007. The Eocene–Oligocene Transition. In: Williams, M., Haywood, A.M., Gregory, F.J., Schmidt, D.N. (Eds.), Deep-Time Perspectives on Climate Change: Marrying the Signal from Computer Models and Biological Proxies. The Micropalaeontological Society, Special Publications. Geol. Soc. Lond., pp. 351–387.

de Bonis, L., Jaeger, J.-J., Coiffait, B., Coiffait, P.-E., 1988. Découverte du plus ancien primate catarrhinien connu dans l'Éocène supérieur d'Afrique du Nord. C. R. Acad. Sci. Paris 306, 929–934.

de Vries, D., Heritage, S., Borths, M.R., Sallam, H.M., Seiffert, E.R., 2021. Widespread loss of mammalian lineage and dietary diversity in the early Oligocene of Afro-Arabia. Commun. Biol. 4, 1172.

Ducrocq, S., Manthi, K.F., Lihoreau, F., 2011. First record of a parapithecid primate from the Oligocene of Kenya. J. Hum. Evol. 61, 327–331.

Egi, N., Takai, M., Shigehara, N., Tsubamoto, T., 2004. Body mass estimates for Eocene eosimiid and amphipithecid primates using prosimian and anthropoid scaling models. Int. J. Primatol. 25, 211–236.

Fabre, P.-H., Tilak, M.-K., Denys, C., Gaubert, P., Nicolas, V., Douzery, E.J.P., Marivaux, L., 2018. Flightless scaly-tailed squirrels never learned how to fly: a reappraisal of Anomaluridae phylogeny. Zool. Scrip. 47, 404–417.

Gagnon, M., 1997. Ecological diversity and community ecology in the Fayum sequence (Egypt). J. Hum. Evol. 32, 133–160.

Geoffroy Saint-Hilaire, E., 1812. Suite au tableau des quadrumanes. Seconde famille, Lémuriens, Strepsirrhini. Ann. Mus. Hist. Nat. Paris 19, 156–170.

Gheerbrant, E., Thomas, H., Roger, J., Sen, S., Al-Sulaimani, Z., 1993. Deux nouveaux primates dans l'Oligocène Inférieur de Taqah (Sultanat d'Oman) : premiers Adapiformes (?Anchomomyini) de la péninsule Arabique ? Palaeovertebrata 22, 141–196.

Gheerbrant, E., Thomas, H., Sen, S., Al-Sulaimani, Z., 1995. Nouveau Primate Oligopithecinae (Simiiformes) de l'Oligocène inférieur de Taqah, Sultanat d'Oman. C. R. Acad. Sci. Paris 321, 425–432.

Gheerbrant, E., Sudre, J., Sen, S., Abrial, C., Marandat, B., Sigé, B., Vianey-Liaud, M., 1998. Nouvelles données sur les mammifères du Thanétien et de l'Yprésien du Bassin d'Ouarzazate (Maroc) et leur contexte stratigraphique. Palaeovertebrata 27, 155–202.

Gingerich, P.D., Sahni, A., 1984. Dentition of *Sivaladapis nagrii* (Adapidae) from the Late Miocene of India. Int. J. Primatol. 5, 63–79.

Ginsburg, L., Mein, P., 1987. *Tarsius thailandica* nov. sp., premier Tarsiidae (Primates, Mammalia) fossile d'Asie. C. R. Acad. Sci. Paris 304, 1213–1215.

Godinot, M., 1998. A summary of adapiform systematics and phylogeny. Folia Primatol. 69, 218–249.

Godinot, M., 2006. Lemuriform origins as viewed from the fossil record. Folia Primatol. 77, 446–464.

Godinot, M., 2010. Paleogene prosimians. In: Werdelin, L., Sanders, W.J. (Eds.), Cenozoic Mammals of Africa. University of California Press, Berkeley, pp. 319–331.

Godinot, M., Mahboubi, M., 1992. Earliest known simian primate found in Algeria. Nature 357, 324–326.

Godinot, M., Mahboubi, M., 1994. Les petits primates simiiformes de Glib Zegdou (Eocène inférieur à moyen d'Algérie). C. R. Acad. Sci. Paris 319, 357–364.

Godinot, M., Senut, B., Pickford, M., 2018. Primitive Adapidae from Namibia sheds light on the early primate radiation in Africa. Comm. Geol. Surv. Namibia 18, 140–162.

Gray, J.E., 1825. Outline of an attempt at the disposition of the Mammalia into tribes and families with a list of the genera apparently appertaining to each tribe. Ann. Phylos. 10, 337–344.

Gregory, W.K., 1915. On the classification and phylogeny of the Lemuroidea. Bull. Geol. Soc. Am. 26, 426–446.

Gunnell, G.F., Boyer, D.M., Friscia, A.R., Heritage, S., Kyalo Manthi, F., Miller, E.R., Sallam, H.M., Simmons, N.B., Stevens, N.J., Seiffert, E.R., 2018. Fossil lemurs from Egypt and Kenya suggest an African origin for Madagascar's aye aye. Nat. Commun. 9, 3193.

Harcourt, C.S., Bearder, S.K., 1989. A comparison of *Galago moholi* in South Africa with *Galago zanzibaricus*. Am. J. Primatol. 10, 339–355.

Harrison, T., 2010. Later Tertiary Lorisiformes (Strepsirrhini, Primates). In: Werdelin, L., Sanders, W.J. (Eds.), Cenozoic Mammals of Africa. University of California Press, Berkeley, pp. 333–349.

Hartenberger, J.-L., Marandat, B., 1992. A new genus and species of an early Eocene Primate from North Africa. Hum. Evol. 7, 9–16.

Hooker, J.J., Russell, D.E., Phelizon, A., 1999. A new family of Plesiadapiformes (Mammalia) from the Old World lower Paleogene. Palaeontology 42, 377–407.

International Commission of Zoological Nomenclature (ICZN), 1999. International Code of Zoological Nomenclature. The International Trust for Zoological Nomenclature, London. http://www.nhm.ac.uk/hosted-sites/iczn/code/

Jaeger, J.-J., Beard, K.C., Chaimanee, Y., Salem, M., Benammi, M., Hlal, O.A., Coster, P., Bilal, A.A., Duringer, P., Schuster, M., Valentin, X., Marandat, B., Marivaux, L., Métais, E., Hammuda, O., Brunet, M., 2010. Late middle Eocene epoch of Libya yields earliest known radiation of African anthropoids. Nature 467, 1095–1098.

Jablonski, N.G., 2003. The evolution of tarsiid niche. In: Wright, P.C., Simons, E.L., Gursky, S. (Eds.), Tarsiers: Past, Present, and Future. Rutgers University Press, New Brunswick, New Jersey, pp. 35–49.

Jablonski, N.G., 2005. Primate homeland: forest and the evolution of primate during the Tertiary and Quaternary in Asia. Anthropol. Sci. 113, 117–122.

Janis, C.M., 1993. Tertiary mammal evolution in the context of changing climates, vegetation, and tectonic events. Annu. Rev. Ecol. Syst. 24, 467–500.

Kappeler, P.M., 1991. Patterns of sexual dimorphism in body weight among prosimian primates. Folia Primatol. 57, 132–146.

Kay, R.F., 1977. The evolution of molar occlusion in the Cercopithecidae and early catarrhines. Am. J. Phys. Anthropol. 46: 327–352.

Kay, R.F., Williams, B.A., 1994. Dental evidence for anthropoid origins. In: Fleagle, J.G., Kay, R.F. (Eds.), Anthropoid Origins. Plenum Press, New York, pp. 361–445.

Kay, R.F., Fleagle, J.G., Simons, E.L., 1981. A revision of the Oligocene apes of the Fayum Province, Egypt. Am. J. Phys. Anthropol. 55: 293–322.

Kay, R.F., Ross, C., Williams, B.A., 1997. Anthropoid origins. Science 275, 797–804.

Kay, R.F., Williams, B.A., Ross, C.F., Takai, M., Shigehara, N., 2004. Anthropoid origins: a phylogenetic analysis. In: Ross, C.F., Kay, R.F. (Eds.), Anthropoid Origins: New Visions. Plenum Press, New York, pp. 91–135.

Köhler, M., Moyà-Solà, S., 1999. A finding of Oligocene primates on the European continent. Proc. Natl. Acad. Sci. USA 96, 14664–14667.

Leakey, M.G., Ungar, P.S., Walker, A., 1995. A new genus of large primate from the Late Oligocene of Lothidok, Turkana District, Kenya. J. Hum. Evol. 28, 519–531.

Linnaeus, C., 1758. *Systema Naturae per Regna Tria Naturae, secundum Classes, Ordines, Genera, Species cum Characteribus, Differentiis, Synomymis, Locis*. Vol. 1: Regnum Animale. Editio Decima, Reformata, Laurentius Salvius, Stockholm.

Marigó, J., Minwer-Barakat, R., Moyà-Solà, S., 2011. New *Anchomomys* (Adapoidea, Primates) from the Robiacian (Middle Eocene) of northeastern Spain. Taxonomic and evolutionary implications. J. Hum. Evol. 60, 665–672.

Marigó, J., Minwer-Barakat, R., Moyà-Solà, S., 2013. *Nievesia sossisensis*, a new anchomomyin (Adapiformes, Primates) from the early Late Eocene of the southern Pyrenees (Catalonia, Spain). J. Hum. Evol. 64, 473–485.

Marivaux, L., 2006. The eosimiid and amphipithecid primates (Anthropoidea) from the Oligocene of the Bugti Hills (Balochistan, Pakistan): new insight into early higher primate evolution in South Asia. Palaeovertebrata 34, 29–109.

Marivaux, L., Boivin, M., 2019. Emergence of hystricognathous rodents (Mammalia, Hystricognathi): Palaeogene fossil record, phylogeny, macroevolution and historical biogeography. Zool. J. Linnean Soc. 187, 929–964.

Marivaux, L., Charruault, A.-L., Benammi, M., 2024. 3D models related to the publication: A new primate community from the earliest Oligocene of the Atlantic margin of Northwest Africa: Systematic, paleobiogeographic and paleoenvironmental implications. MorphoMuseuM, in press. https://doi.org/10.18563/journal.m3.208

Marivaux, L., Welcomme, J.-L., Ducrocq, S., Jaeger, J.-J., 2002. Oligocene sivaladapid primate from the Bugti Hills (Balochistan, Pakistan) bridges the gap between Eocene and Miocene adapiform communities in southern Asia. J. Hum. Evol. 42, 379–388.

Marivaux, L., Adnet, S., Benammi, M., Tabuce, R., Yans, J., Benammi, M., 2017a. Earliest Oligocene hystricognathous rodents from the Atlantic margin of Northwestern Saharan Africa (Dakhla, Morocco): systematic, paleobiogeographical and paleoenvironmental implications. J. Vert. Paleontol. 37, e1357567.

Marivaux, L., Adnet, S., Benammi, M., Tabuce, R., Benammi, M., 2017b. Anomaluroid rodents from the earliest Oligocene of Dakhla, Morocco, reveal the long-lived and morphologically conservative pattern of the Anomaluridae and Nonanomaluridae during the Tertiary in Africa. J. Syst. Palaeontol. 15, 539–569.

Marivaux, L., Boivin, M., Adnet, S., Benammi, M., Tabuce, R., Benammi, M., 2019. Incisor enamel microstructure of hystricognathous and anomaluroid rodents from the earliest Oligocene of Dakhla, Atlantic Sahara (Morocco). J. Mamm. Evol. 26, 373–388.

Marivaux, L., Welcomme, J.-L., Antoine, P.-O., Métais, G., Baloch, I.M., Benammi, M., Chaimanee, Y., Ducrocq, S., Jaeger, J.-J., 2001. A fossil lemur from the Oligocene of Pakistan. Science 294, 587–591.

Marivaux, L., Bocat, L., Chaimanee, Y., Jaeger, J.-J., Marandat, B., Srisuk, P., Tafforeau, P., Yamee, C., Welcomme, J.-L., 2006. Cynocephalid dermopterans from the Palaeogene of South Asia (Thailand, Myanmar, and Pakistan): systematic, evolutionary and paleobiogeographic implications. Zool. Scrip. 35, 395–420.

Marivaux, L., Ramdarshan, A., Essid, E.M., Marzougui, W., Khayati Ammar, H., Lebrun, R., Marandat, B., Merzeraud, G., Tabuce, R., Vianey-Liaud, M., 2013. *Djebelemur*, a tiny pre-tooth-combed primate from the Eocene of Tunisia: a glimpse into the origin of crown strepsirhines. PLoS ONE 8, e80778.

Marivaux, L., Essid, E.M., Marzougui, W., Khayati Ammar, H., Adnet, S., Marandat, B., Merzeraud, G., Ramdarshan, A., Tabuce, R., Vianey-Liaud, M., Yans, Y., 2014. A morphological intermediate between eosimiiform and simiiform primates from the late middle Eocene of Tunisia: macroevolutionary and paleobiogeographic implications of early anthropoids. Am. J. Phys. Anthropol. 154, 387–401.

Marivaux, L., Antoine, P.-O., Baqri, S.R.H., Benammi, M., Chaimanee, Y., Crochet, J.-Y., De Franceschi, D., Iqbal, N., Jaeger, J.-J., Métais, G., Roohi, G., Welcomme, J.-L., 2005. Anthropoid primates from the Oligocene of Pakistan (Bugti Hills): data on early anthropoid evolution and biogeography. Proc. Natl. Acad. Sci. USA 102, 8436–8441.

Marivaux, L., Negri, F.R., Antoine, P.-O., Stutz, N., Condamine, F.L., Kerber, L., Pujos, F., Ventura Santos, R., Alvim, A.M.V., Hsiou, A.S., Bissaro Júnior, M.C., Adami-Rodrigues, K., Ribeiro, A.M., 2023. An eosimiid primate of South Asian affinities in the Paleogene of Western Amazonia and the origin of New World monkeys. Proc. Natl. Acad. Sci. USA 120, e2301338120.

Mattingly, S.G., Beard, K.C., Coster, P.M.C., Salem, M.J., Chaimanee, Y., Jaeger, J.-J., 2021. A new parapithecine (Primates: Anthropoidea) from the early Oligocene of Libya supports parallel evolution of large body size among parapithecids. J. Hum. Evol. 153, 102957.

Meng, J., McKenna, M.C., 1998. Faunal turnovers of Palaeogene mammals from the Mongolian Plateau. Nature 394, 364–367.

Mittermeier, R.A., Tattersall, I., Konstant, B., Meyers, D.M., Mast, R.B. (Eds.), 1994. Lemurs of Madagascar. Conservation International, Washington D.C.

Mivart, St G., 1864. Notes on the crania and dentition of the Lemuridae. Proc. Zool. Soc. Lond. 1918, 611–648.

Ni, X., Li, Q., Li, L., Beard, K.C., 2016. Oligocene primates from China reveal divergence between African and Asian primate evolution. Science 352, 673–677.

Ni, X., Gebo, D.L., Dagosto, M., Meng, J., Tafforeau, P., Flynn, J.J., Beard, K.C., 2013. The oldest known primate skeleton and early haplorhine evolution. Nature 498, 60–64.

Noiret, C., Benammi, M., Adnet, S., Enault, S., Marivaux, L., Tabuce, R., Surault, J., Baidder, L., Saddiqi, O., El Kati, I., Benammi, M., Yans, J., 2017. Carbon isotope chemostratigraphy on organics (δ13Corg): a powerful tool to refine the Paleogene age of the fossil-bearing levels in the Dakhla area (Southwestern Moroccan Sahara). The First West African Craton and Margins International Workshop (WACMA1), April 24-29th, 2017, Dakhla, Morocco, pp. 79–80.

Osborn, H.F., 1908. New fossil mammals from the Fayûm Oligocene, Egypt. Am. Mus. Nat. Hist. Bull. 26, 415–424.

Pickford, M., 1986. Première découverte d'une faune mammalienne terrestre paléogène d'Afrique sub-saharienne. C. R. Acad. Sci. Paris 302, 1205–1210.

Pickford, M., Senut, B., Morales, J., Mein, P., Sanchez, I.M., 2008. Mammalia from the Lutetian of Namibia. Memoir Geol. Surv. Namibia 20, 465–514.

Pocock, R.I., 1918. On the external characters of the lemurs and of *Tarsius*. Proc. Zool. Soc. Lond. 88, 19–53.

Qi, T., Beard, K.C., 1998. Late Eocene sivaladapid primate from Guangxi Zhuang Autonomous Region People's Republic of China. J. Hum. Evol. 35, 211–220.

Rasmussen, D.T., Simons, E.L., 1988. New specimens of *Oligopithecus savagei*, early Oligocene primate from the Fayum, Egypt. Folia Primatol. 51, 182–208.

Rasmussen, D.T., Bown, T.M., Simons, E.L., 1992. The Eocene-Oligocene transition in continental Africa. In: Prothero, D.R., Berggren, W.A. (Eds.), Eocene-Oligocene Climatic and Biotic Evolution. Princeton University, Princeton, New Jersey, pp. 548–566.

Rosenberger, A.L., Klukkert, Z.S., Cook, S.B., Rimoli, R., 2013. Rethinking *Antillothrix*: the mandible and its implications. Am. J. Primatol. 75, 825–836.

Ross, C., Williams, B., Kay, R.F., 1998. Phylogenetic analysis of anthropoid relationships. J. Hum. Evol. 35, 221–306.

Rust, K., Ni, X., Tietjen, K., Beard, K.C., 2023. Phylogeny and paleobiogeography of the enigmatic North American primate *Ekgmowechashala* illuminated by new fossils from Nebraska (USA) and Guangxi Zhuang Autonomous Region (China). J. Hum. Evol. 183, 103452.

Savage, D.E., Russell, D.E., 1983. Mammalian Paleofaunas of the World. Addison-Wesley, Reading, MA.

Schlösser, M., 1910. Über einige fossile Säugetiere aus dem Oligocän von Ägypten. Zool. Anz. 34, 500–508.

Schlösser, M., 1911. Beiträge zur Kenntnis der oligozänen Landsäugetiere aus dem Fayum, Ägypten. Beitr. Pal. Geol. Osterr. - Ung. 24, 51–167.

Schwartz, J.H., Tattersall, I., 1985. Evolutionary relationships of living lemurs and lorises (Mammalia, Primates) and their potential affinities with European Eocene Adapidae. Anthropol. Pap. Am. Mus. Nat. Hist. 60, 1–100.

Seiffert, E.R., 2006. Revised age estimates for the later Paleogene mammal faunas of Egypt and Oman. Proc. Natl. Acad. Sci. USA 103, 5000–5005.

Seiffert, E.R., 2007a. Evolution and extinction of Afro-Arabian Primates near the Eocene-Oligocene boundary. Folia Primatol. 78, 314–327.

Seiffert, E.R., 2007b. Early evolution and biogeography of lorisiform strepsirrhines. Am. J. Primatol. 69, 27–35.

Seiffert, E.R., 2012. Early primate evolution in Afro-Arabia. Evol. Anthropol. 21, 239–253.

Seiffert, E.R., Simons, E.L., 2001. Astragalar morphology of late Eocene anthropoids from the Fayum Depression (Egypt) and the origin of catarrhine primates. J. Hum. Evol. 41, 577–606.

Seiffert, E.R., Simons, E.L., Attia, Y., 2003. Fossil evidence of lorises and galagos. Nature 422, 421–424.

Seiffert, E.R., Simons, E.L., Ryan, T.M., Attia, Y., 2005b. Additional remains of *Wadilemur elegans*, a primitive stem galagid from the late Eocene of Egypt. Proc. Natl. Acad. Sci. USA 102, 11396–11401.

Seiffert, E.R., Perry, J.M.G., Simons, E.L., Boyer, D.M., 2009. Convergent evolution of anthropoid-like adaptations in Eocene adapiform primates. Nature 461, 1118–1122.

Seiffert, E.R., Simons, E.L., Fleagle, J.G., Godinot, M., 2010. Paleogene anthropoids. In: Werdelin, L., Sanders, W.J. (Eds.), Cenozoic Mammals of Africa. University of California Press, Oakland, pp. 369–392.

Seiffert, E.R., Boyer, D.M., Fleagle, J.G., Gunnell, G.F., Heesy, C.P., Perry, J.M.G., Sallam, H.M., 2018. New adapiform primate fossils from the late Eocene of Egypt. Hist. Biol. 30, 204–226.

Seiffert, E.R., Simons, E.L., Clyde, W.C., Rossie, J.B., Attia, Y., Bown, T.M., Chatrath, P., Mathison, M.E., 2005a. Basal anthropoids from Egypt and the antiquity of Africa's higher primate radiation. Science 310, 300–304.

Seiffert, E.R., Tejedor, M.F., Fleagle, J.G., Novo, N.M., Cornejo, F.M., Bond, M., de Vries, D., Campbell Jr, K.E., 2020. A parapithecid stem anthropoid of African origin in the Paleogene of South America. Science 368, 194–197.

Sigé, B., Jaeger, J.-J., Sudre, J., Vianey-Liaud, M., 1990. *Altiatlasius koulchii* n. gen. et sp., primate omomyidé du Paléocène supérieur du Maroc, et les origines des Euprimates. Palaeontographica 214, 31–56.

Simons, E.L., 1962. Two new primate species from the African Oligocene. Postilla 64, 1–12.

Simons, E.L., 1965. New fossil apes from Egypt and the initial differentiation of Hominoidea. Nature 205, 135–139.

Simons, E.L., 1974. *Parapithecus grangeri* (Parapithecidae, Old World higher primates): new species from the Oligocene of Egypt and the initial differentiation of Cercopithecoidea Postilla 166, 1–12.

Simons, E.L., 1989. Description of two genera and species of Late Eocene Anthropoidea from Egypt. Proc. Natl. Acad. Sci. USA 86, 9956–9960.

Simons, E.L., 1990. Discovery of the oldest known anthropoidean skull from the Paleogene of Egypt. Science 247, 1567–1569.

Simons, E.L., 1992. Diversity in the early Tertiary anthropoidean radiation in Africa. Proc. Natl. Acad. Sci. USA 89, 10743–10747.

Simons, E.L., 1995a. Skulls and anterior teeth of *Catopithecus* (Primates, Anthropoidea) from the Eocene and anthropoid origins. Science 268, 1885–1888.

Simons, E.L., 1995b. Crania of *Apidium*: primitive anthropoidean (primates, Parapithecidae) from the Egyptian Oligocene Am. Mus. Novitates 3124, 1–10.

Simons, E.L., 1997. Preliminary description of the cranium of *Proteopithecus sylviae*, an Egyptian Late Eocene anthropoidean primate. Proc. Natl. Acad. Sci. USA 94, 14970–14975.

Simons, E.L., Bown, T.M., 1985. *Afrotarsius chatrathi*, first tarsiiform primate (? Tarsiidae) from Africa. Nature 313, 475–477.

Simons, E., Kay, R.F., 1983. *Qatrania*, new basal anthropoid primate from the Fayum, Oligocene of Egypt. Nature 304, 624–626.

Simons, E., Kay, R.F., 1988. New material of *Qatrania* from Egypt with comments on the phylogenetic position of the Parapithecidae (primates, Anthropoidea). Am. J. Phys. Anthropol. 15, 337–347.

Simons, E.L., Rasmussen, D.T., 1994. A remarkable cranium of *Plesiopithecus teras* (Primates, Prosimii) from the Eocene of Egypt. Proc. Natl. Acad. Sci. USA 91, 9946–9950.

Simons, E.L., Rasmussen, D.T., 1996. Skull of *Catopithecus browni*, an early Tertiary catarrhine. Am. J. Phys. Anthropol. 100, 261–292.

Simons, E.L., Miller, E.R., 1997. An upper dentition of *Afromonius dieides* (Primates) from the Fayum, Egyptian Eocene. Proc. Natl. Acad. Sci. USA 94, 7993–7996.

Simons, E.L., Rasmussen, D.T., Gebo, D.L., 1987. A new species of *Propliopithecus* from the Fayum, Egypt. Am. J. Phys. Anthropol. 73, 139–148.

Simons, E.L., Rasmussen, D.T., Gingerich, P.D., 1995. New cercamoniine adapid from Fayum, Egypt. J. Hum. Evol. 29, 577–589.

Simons, E.L., Rasmussen, D.T., Bown, T.M., Chatrath, P.S., 1994. The Eocene origin of anthropoid primates: adaptation, evolution, and diversity. In: Fleagle, J.G., Kay, R.F. (Eds.), Anthropoid Origins. Plenum Press, New York, pp. 179–201.

Simons, E.L., Seiffert, E.R., Chatrath, P.S., Attia, Y., 2001. Earliest record of a parapithecid anthropoid from the Jebel Qatrani Formation, Northern Egypt. Folia Primatol. 72, 316–331.

Simpson, G.G., 1967. The Tertiary lorisiform primates of Africa. Bull. Mus. Comp. Zool. 136, 39–62.

Smith, R.J., 1993. Logarithmic transformation bias in allometry. Am. J. Phys. Anthropol. 90, 215–228.

Stehlin, H.G., 1909. Remarques sur les faunules de mammifères des couches éocènes et oligocènes du Basin de Paris. Bull. Soc. Geol. France 9, 488–520.

Stehlin, H.G., 1916. Die Säugetiere des schweizerischen Eocäens. Critischer Catalog der Materialen. Abh. schweiz. Pal. Ges. 41, 1299–1552.

Stevens, N.J., Seiffert, E.R., O'Connor, P.M., Roberts, E.M., Schmidz, M.D., Krause, C., Gprscak, E., Ngasala, S., Hieronymus, T.L., Temu, J., 2013. Palaeontological evidence for an Oligocene divergence between Old World monkeys and apes. Nature 497, 611–614.

Strauss, W.L.J., 1961. Primate taxonomy and *Oreopithecus*. Science 133, 760–761.

Sudre, J., 1975. Un prosimien du Paléogène ancien du Sahara nord occidental : *Azibius trerki* n. g. n. sp. C. R. Acad. Sci. Paris 280, 1539–1542.

Szalay, F.S., Delson, E., 1979. Evolutionary History of the Primates. Academic Press, New York.

Tabuce, R., Mahboubi, M., Tafforeau, P., Sudre, J., 2004. Discovery of a highly-specialized plesiadapiform primate in the early-middle Eocene of northwestern Africa. J. Hum. Evol. 47, 305–321.

Tabuce, R., Adnet, S., Cappetta, H., Noubhani, A., Quillevéré, F., 2005. Aznag (bassin d'Ouarzazate, Maroc), nouvelle localité à sélaciens et mammifères de l'Eocène moyen (Lutétien) d'Afrique. Bull. Soc. Geol. France 176, 381–400.

Tabuce, R., Marivaux, L., Lebrun, R., Adaci, M., Bensalah, M., Fabre, P.-H., Fara, E., Gomes Rodrigues, H., Hautier, L., Jaeger, J.-J., Lazzari, V., Mebrouk, F., Peigné, S., Sudre, J., Tafforeau, P., Valentin, X., Mahboubi, M., 2009. Anthropoid vs. strepsirhine status of the African Eocene primates *Algeripithecus* and *Azibius*: craniodental evidence. Proc. Roy. Soc. Lond. B 276, 4087–4094.

Takai, M., 1994. New specimens of *Neosaimiri fieldsi* from La Venta, Colombia: a middle Miocene ancestor of the living squirrel monkeys. J. Hum. Evol. 27, 329–360.

Thomas, H., Roger, J., Sen, S., Al-Sulaimani, Z., 1988. Découverte des plus anciens "Anthropoïdes" du continent arabo-africain et d'un Primate tarsiiforme dans l'Oligocène du Sultanat d'Oman. C. R. Acad. Sci., Paris 306, 823–829.

Thomas, H., Sen, S., Roger, J., Al-Sulaimani, Z., 1991. The discovery of *Moeripithecus markgrafi* Schlösser (Propliopithecidae, Anthropoidea, Primates), in the Ashawq Formation (early Oligocene of Dhofar Province, Sultanate of Oman). J. Hum. Evol. 20, 33–49.

Thomas, H., Roger, J., Sen, S., Al-Sulaimani, Z., 1992. Early Oligocene vertebrates from Dhofar (Sultanate of Oman). In: Sadek, A. (Ed.), Geology of the Arab World. Cairo University, Cairo, pp. 283–293.

Tramoy, R., Salpin, M., Schnyder, J., Person, A., Sebilo, M., Yans, J., Vaury, V., Fozzani, J., Bauer, H., 2016. Stepwise palaeoclimate change across the Eocene–Oligocene transition recorded in continental NW Europe by mineralogical assemblages and d15Norg (Rennes Basin, France). Terra Nova 28, 212–220.

Weppe, R., Condamine, F.L., Guinot, G., Maugoust, J., Orliac, M.J., 2023. Drivers of the artiodactyl turnover in insular Western Europe at the Eocene–Oligocene Transition. Proc. Natl. Acad. Sci. USA 120, e2309945120.

Westerhold, T., Marwan, N., Drury, A.J., Liebrand, D., Agnini, C., Anagnostou, E., Barnet, J.S.K., Bohaty, S.M., De Vleeschouwer, D., Florindo, F., Frederichs, T., Hodell, D.A., Holbourn, A.E., Kroon, D., Lauretano, V., Littler, K., Lourens, L.J., Lyle, M., Pälike, H., Röhl, U., Tian, J., Wilkens, R.H., Wilson, P.A., Zachos, J.C., 2020. An astronomically dated record of Earth's climate and its predictability over the last 66 million years. Science 369, 1383–1387.

Zachos, J.C., Dickens, G.R., Zeebe, R.E., 2008. An early Cenozoic perspective on greenhouse warming and carbon-cycle dynamics. Nature 451, 279–283.

Zalmout, I.S., Sanders, W.J., MacLatchy, L.M., Gunnell, G.F., Al-Mufarreh, Y.A., Ali, M.A., Nasser, A.A.H., Al-Masari, A.M., Al-Sobhi, S.A., Nadhra, A.O., Matari, A.H., Wilson, J.A., Gingerich, P.D., 2010. New Oligocene primate from Saudi Arabia and the divergence of apes and Old World monkeys. Nature 466, 360–364.

Zanazzi, A., Kohn, M.J., MacFadden, B.J., Terry, D.O., 2007. Large temperature drop across the Eocene-Oligocene transition in Central North America. Nature 445, 639–642.

Table 1. Dental measurements (in mm) and adult body mass estimates (in grams) for primate specimens from DAK C_2. (MDL, maximum mesiodistal length; BLW, maximum buccolingual width; BM, body mass).

		MDL	BLW	BM
Haplorhini				
Anthropoidea				
Oligopithecidae				
Catopithecus aff. *browni*				
DAK-Arg-090	left P^4	2,25	3,80	~ 906
DAK-Pto-053	right M^1 (lacking the buccal region)	3,63	-	-
DAK-Arg-091	left M^2 (worn)	3,67	4,91	~ 2060
DAK-Arg-089	left M_1 (worn)	4,06	3,02	~1390
DAK-Pto-052	right M_1 (pristine but lacking the mesiobuccal region)	3,71*	3,12	~ 1268
DAK-Arg-087	right M_3	3,77	2,23	~ 920
DAK-Arg-088	right M_2 (abraded)	3,37	2,50	~ 1385
Propliopithecidae				
?*Propliopithecus* sp.				
DAK-Pto-056	right M_3 (fragment of talonid of a germ)	3,91*	3,28*	-
Parapithecidae				
Abuqatrania cf. *basiodontos*				
DAK-Arg-094	left M^2 (corroded, lacking the enamel cap [exposed dentine])	2,31	2,91	-
DAK-Arg-101	left M^3 (abraded)	1,28	2,36	~ 561
DAK-Arg-092	left C_1	1,85	1,40	-
DAK-Arg-095	right I_2 or I_1	1,32	1,48	-
DAK-Arg-096	right P_2 (worn apex)	2,04	1,76	-
DAK-Arg-097	right P_2 (worn apex and broken root)	1,56	1,32	-
DAK-Arg-093	right M_1	2,41	2,24	~ 371
Afrotarsiidae				
Afrotarsius sp.				
DAK-Arg-098	left P_3	1,38	1,20	~ 147
DAK-Pto-054	right M_1 (abraded/corroded)	2,07	1,56	~ 162
Strepsirrhini				
Djebelemuridae				
cf. 'Anchomomys' *milleri*				
DAK-Arg-100	right C_1	1,11	1,36	-
Lorisiformes				
Galagidae				

Wadilemur cf. *elegans*				
DAK-Arg-103	right M^1 or M^2 (lacking the mesial and buccal regions)	2,40*	-	-
DAK-Arg-099	right M_2	2,14	1,48	~ 155
?Lorisiformes				
Orogalago saintexuperyi gen. et sp. nov.				
DAK-Arg-102	left M_2	2,40	2,05	~ 290
Strepsirrhini indet.				
Orolemur mermozi gen. et sp. nov.				
DAK-Pto-055	right M^1 or M^2	2,06	2,42	160-163

* broken specimen

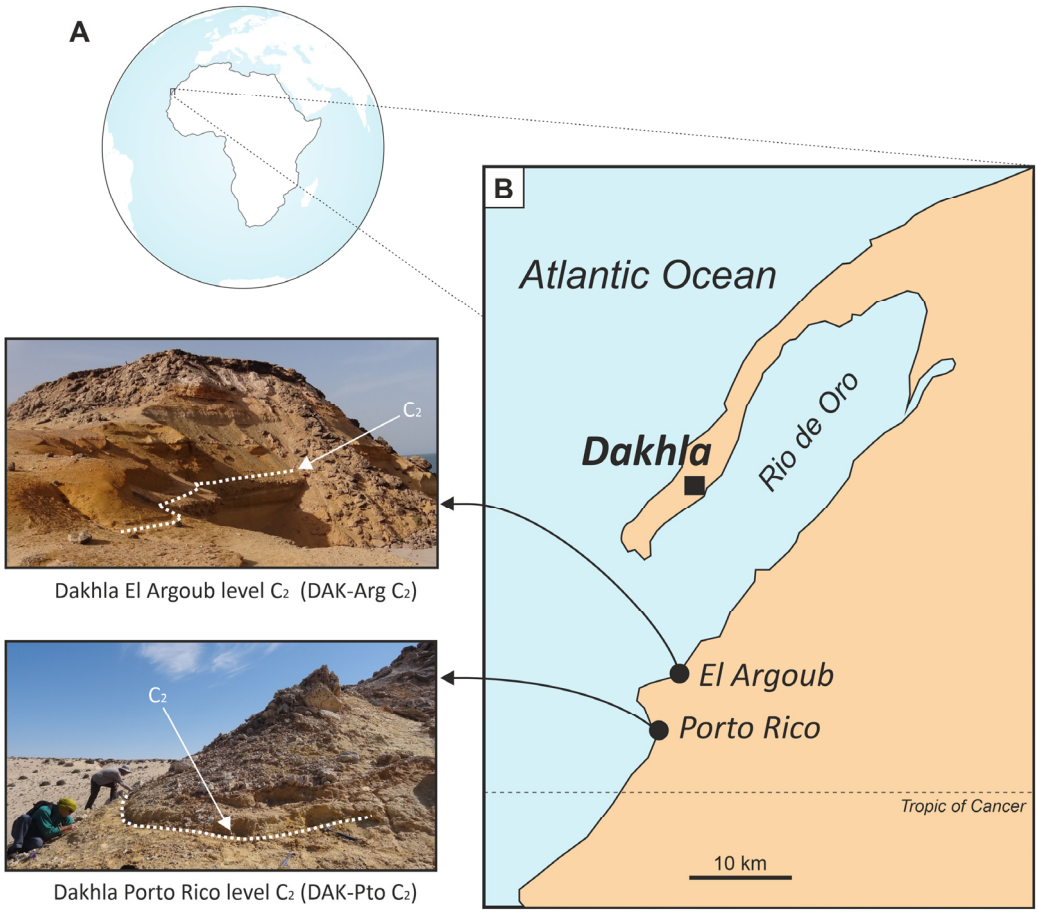

Figure 1. Geographic locations of the primate-yielding localities from lower Oligocene deposits on the Atlantic margin of Northwest Africa (current Dakhla region). **A**, simplified globe centered on Africa, locating the Dakhla peninsula and the *Rio de Oro* in the westernmost part of the Sahara (Atlantic Sahara; in the south of Morocco, near the northern border of Mauritania); **B**, location of the geological outcrops of interest (Porto Rico [Pto] and El Argoub [Arg]), which are exposed on the mainland shore of the *Rio de Oro* inlet, east of the peninsula. The fossil-bearing localities, Porto Rico U4 level C_2 (DAK-Pto C_2) and El Argoub U4 level C_2 (DAK-Arg C_2), are situated directly east of the Dakhla city (ca. 13 km and ca. 10 km, respectively). On the two photographs (by L.M.), the dashed white lines indicate the fossil-bearing level C_2, which consists of a ~30 cm thick unconsolidated sandy microconglomerate. In both sections (Pto and Arg), this level has yielded a similar fossil assemblage of marine and estuarine invertebrates (lamellibranches) and vertebrates (including fishes, turtles, crocodiles, and abundant elasmobranchs), together with terrestrial mammals (Marivaux et al., 2017a, b, 2019; Benammi et al., 2019).

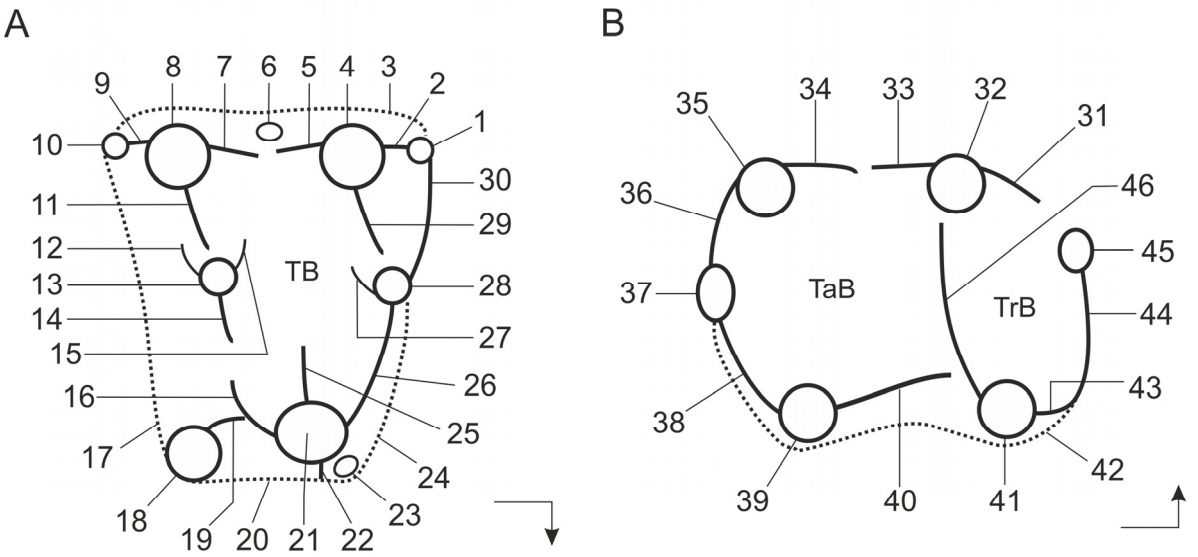

Figure 2. Dental nomenclature. A–B, Schematic occlusal dental morphology of upper (A) and lower (B) teeth of primates and related nomenclature (used for the selected characters of the phylogenetic analyses). The dental terminology is after Marivaux et al. (2023), modified after Kay (1977), Szalay and Delson (1979), and Marivaux (2006). The arrows situated in front of the molars indicate the orientation of the teeth on the jaws (mesiolingual). Upper molars: 1, parastyle; 2, preparacrista; 3, buccal cingulum; 4, paracone; 5, postparacrista; 6, mesostyle; 7, premetacrista; 8, metacone; 9, postmetacrista; 10, metastyle (or metastylar shelf); 11, hypometacrista; 12, postmetaconule crista; 13, metaconule; 14, hypometaconule crista (= metacrista or crista obliqua); 15, premetaconule crista; 16, postprotocrista; 17, distal cingulum; 18, hypocone; 19, prehypocrista; 20, lingual cingulum; 21, protocone; 22, entoprotocrista; 23, pericone; 24, mesial cingulum; 25, endoprotocrista; 26, preprotocrista; 27, postparaconule crista; 28, paraconule; 29, hypoparacrista; 30, preparaconule crista; TB, trigon basin; 2 + 5 + 7 + 9, eocrista; 11 + 14, hypometacrista/metacrista complex (or hypometacrista complex). Lower molars: 31, premetacristid; 32, metaconid; 33, postmetacristid; 34, pre-entocristid; 35, entoconid; 36, postentocristid; 37, hypoconulid; 38, hypocristid; 39, hypoconid; 40, cristid obliqua; 41, protoconid; 42, buccal cingulid; 43, buccal paracristid (or preprotocristid); 44, mediolingual paracristid; 45, paraconid; 46, protocristid (often composed of lateral and medial branches); TaB, talonid basin; TrB, trigonid basin.

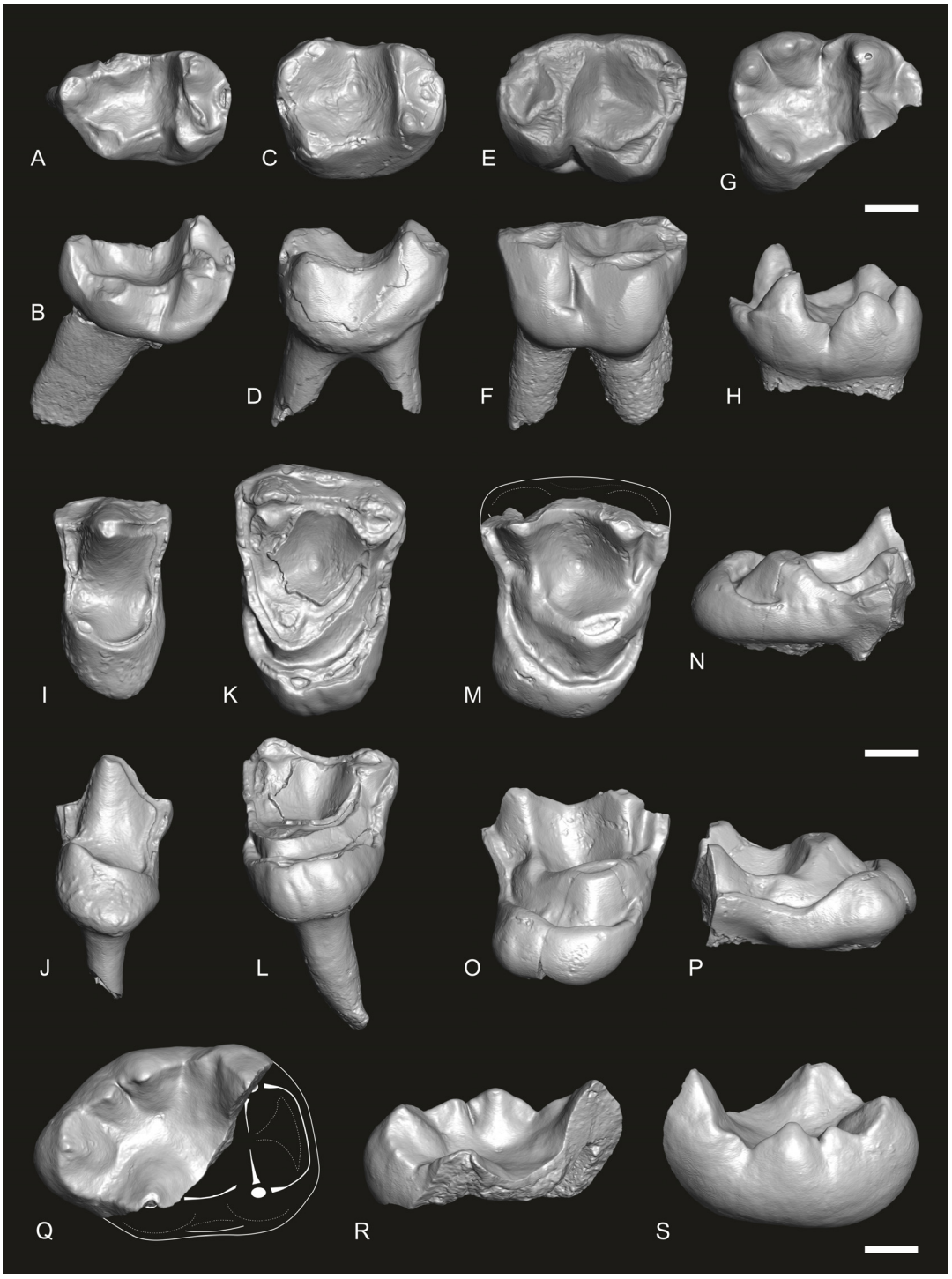

Figure 3. Dental remains of simiiform anthropoid primates (Oligopithecidae and Propliopithecidae) from the earliest Oligocene of Dakhla (DAK-Arg C_2 and DAK-Pto C_2). **A–P**, Oligopithecidae, *Catopithecus* aff. *browni*: DAK-Arg-087, right M_3 in occlusal (A) and buccal (B) views; DAK-Arg-088, right M_2 in occlusal (C) and buccal (D) views; DAK-Arg-089, left M_1 in occlusal (E) and buccal (F) views; DAK-Pto-052, right M_1 in occlusal (G) and lingual (H) views; DAK-Arg-090, left P^4 in occlusal (I) and lingual (J) views; DAK-Arg-091, left M^2 in occlusal (K) and lingual (L) views; DAK-Pto-053, right M^1 in occlusal (M), mesial (N), lingual (O) and distal (P) views. **Q–S**, Propliopithecidae, ?*Propliopithecus* sp.: DAK-Pto-056, right M_3 (fragment of talonid) in occlusal (Q), buccal (R) and lingual (S) views. Images are renderings of 3D digital models of the fossil specimens, obtained by X-ray micro-computed (µCT) surface reconstructions (segmented enamel surfaces). The white lines (solid or dashed) drawn on some specimens (M and Q) are tentative reconstructions of missing tooth parts, based on homologous dental loci of closely related species. Scale bars = 1 mm.

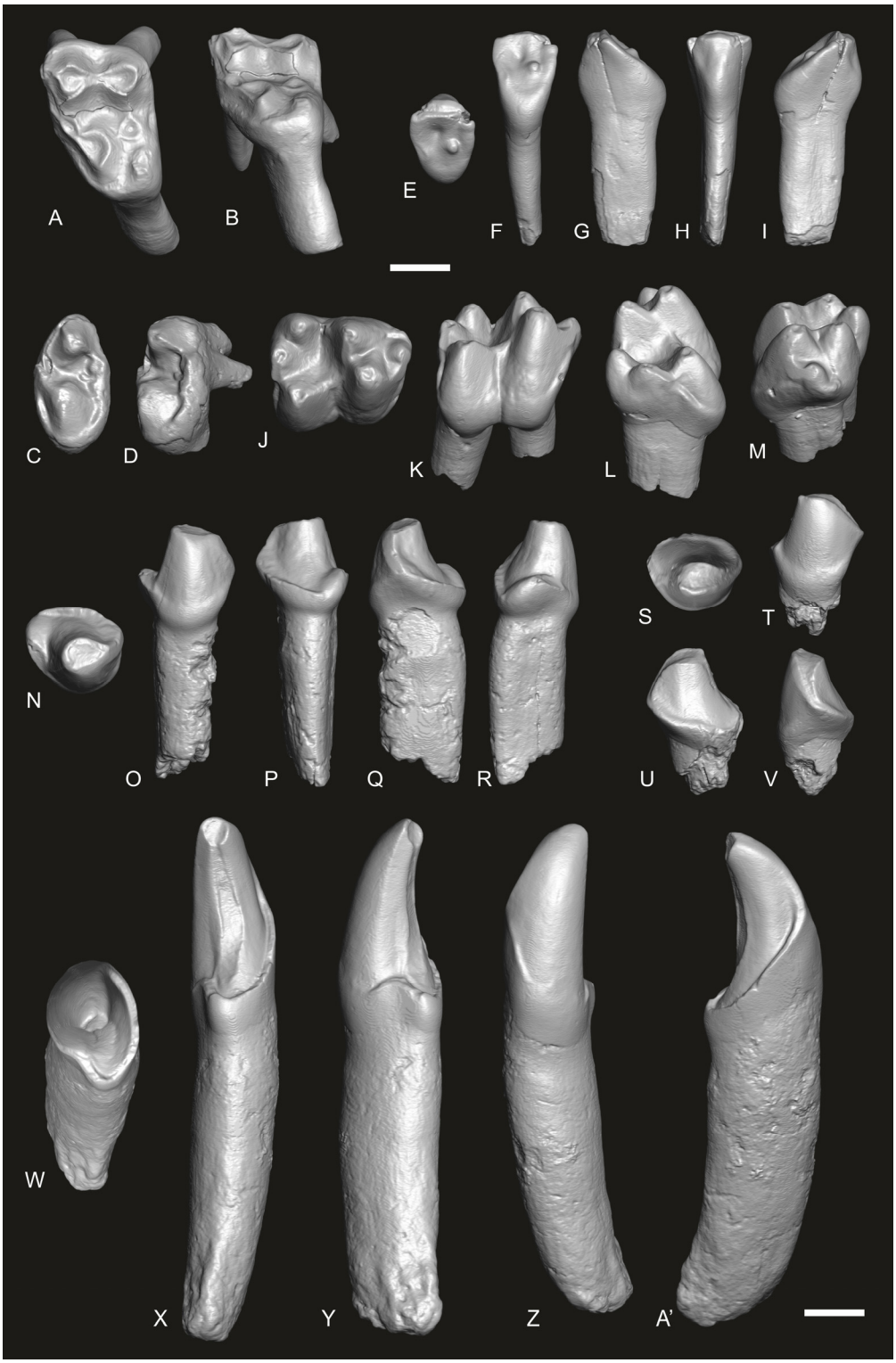

Figure 4. Dental remains of a simiiform anthropoid primate (Parapithecidae) from the earliest Oligocene of Dakhla (DAK-Arg C_2). **A–A'**, *Abuqatrania* cf. *basiodontos*: DAK-Arg-094, left M^1 or M^2 (corroded, lacking the enamel cap) in occlusal (A) and lingual (B) views; DAK-Arg-101, left M^3 (abraded) in occlusal (C) and oblique distal (D) views; DAK-Arg-095, right I_1 or I_2 in occlusal (E), lingual (F), distal (G), buccal (H) and mesial (I) views; DAK-Arg-093, right M_1 in occlusal (J), buccal (K), distal (L) and mesial (M) views; DAK-Arg-096, right P_2 in occlusal (N), buccal (O), lingual (P), mesial (Q) and distal (R) views; DAK-Arg-097, right P_2 in occlusal (S), buccal (T), lingual (U) and mesial (V) views; DAK-Arg-092, left C_1 in occlusal (W), lingual (X), mesial (Y), buccal (Z) and distal (A') views. Images are renderings of 3D digital models of the fossil specimens, obtained by X-ray micro-computed (µCT) surface reconstructions (segmented enamel surfaces). Scale bars = 1 mm.

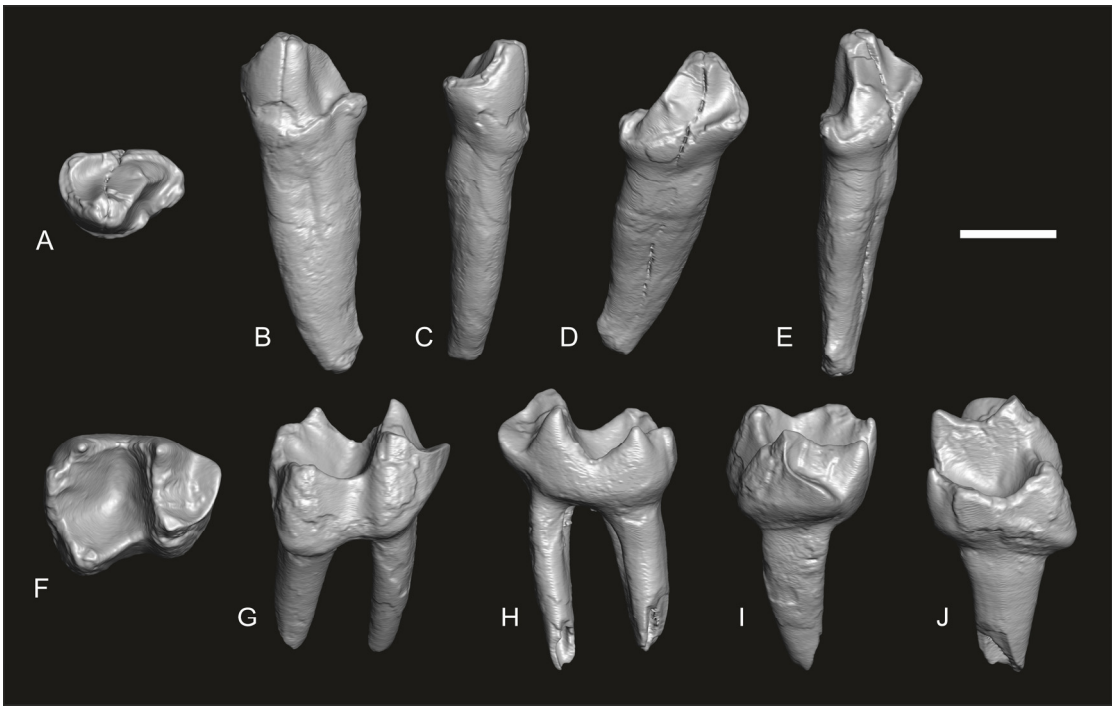

Figure 5. Dental remains of an eosimiiform anthropoid primate (Afrotarsiidae) from the earliest Oligocene of Dakhla (DAK-Arg C_2 and DAK-Pto C_2). **A–J**, *Afrotarsius* sp.: DAK-Arg-098, left P_3 in occlusal (A), buccal (B), mesial (C), lingual (D) and distal (E) views; DAK-Pto-054, right M_1 in occlusal (F), buccal (G), lingual (H), mesial (I) and distal (J) views. Images are renderings of 3D digital models of the fossil specimens, obtained by X-ray micro-computed (µCT) surface reconstructions (segmented enamel surfaces). Scale bar = 1 mm.

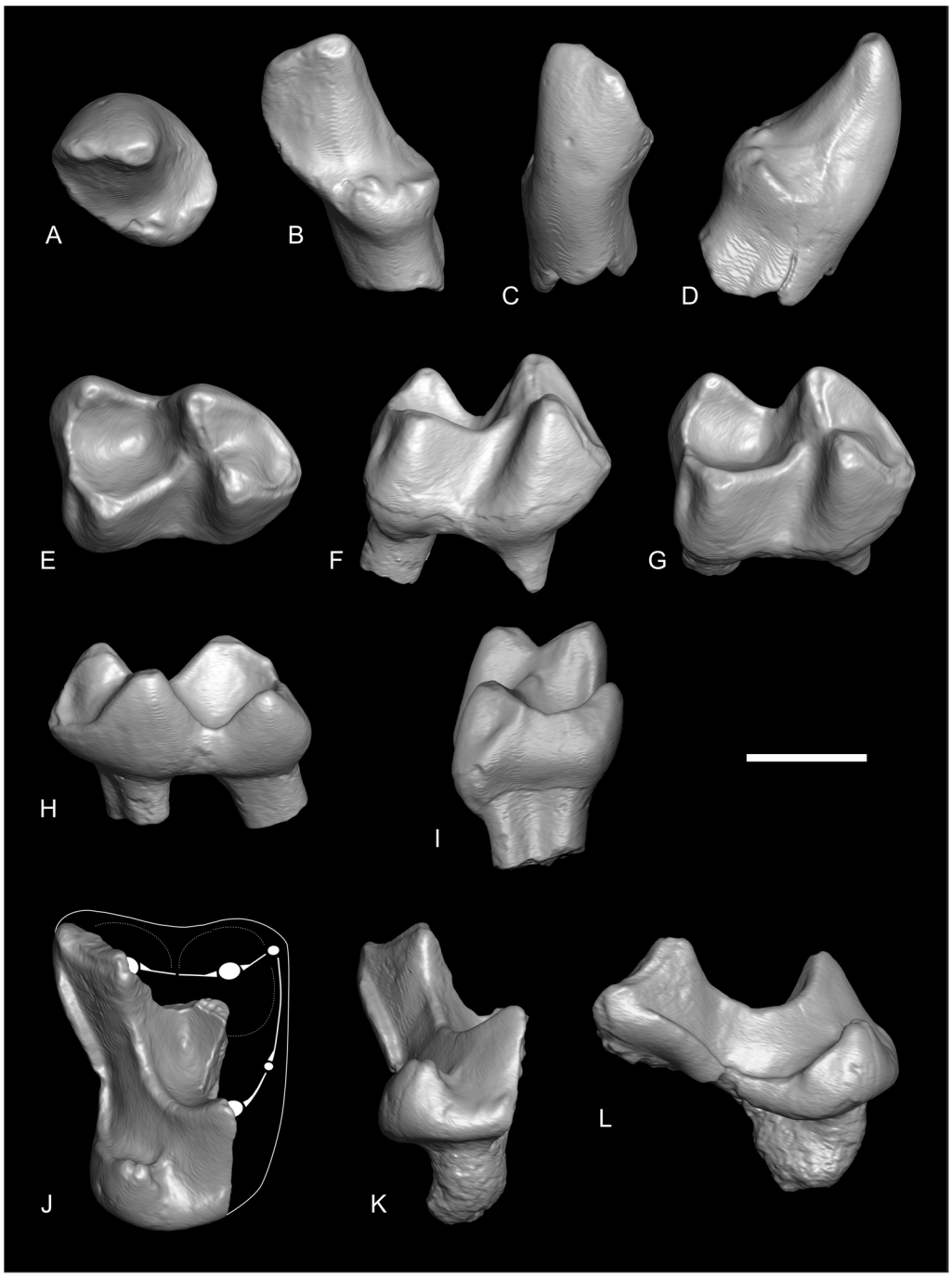

Figure 6. Dental remains of strepsirrhine primates (Djebelemuridae and Galagidae) from the earliest Oligocene of Dakhla (DAK-Arg C_2). **A–D**, cf. '*Anchomomys*' *milleri*: DAK-Arg-100, right C_1 in occlusal (A), lingual (B), buccal (C) and distal (D) views. **E–L**, *Wadilemur* cf. *elegans*: DAK-Arg-099, right M_2 in occlusal (E), buccal (F), semi-buccal (G), lingual (H) and distal (I) views; DAK-Arg-103, right M^1 or M^2 in occlusal (J), lingual (K) and distal (L) views. Images are renderings of 3D digital models of the fossil specimens, obtained by X-ray micro-computed (µCT) surface reconstructions (segmented enamel surfaces). Scale bar = 1 mm. The white lines (solid or dashed) drawn on the DAK-Arg-103 M^1 or M^2 (J) represent a tentative reconstruction of the missing buccal and mesial parts of this tooth, based on the upper molars of *Wadilemur elegans* (Seiffert et al., 2005b, fig. 1A).

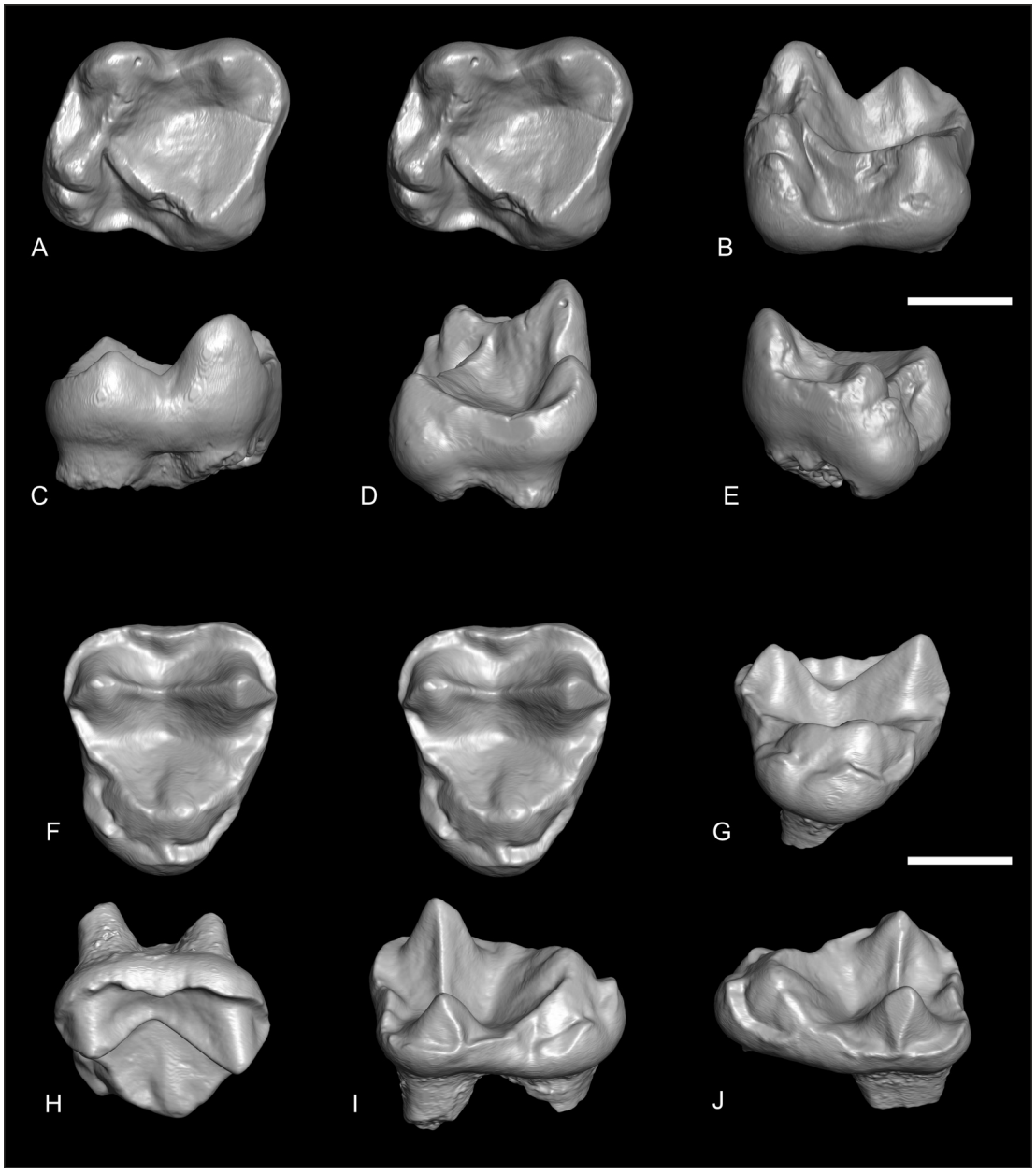

Figure 7. Dental remains of strepsirrhine primates (?Lorisiformes and Strepsirrhini indet.) from the earliest Oligocene of Dakhla (DAK-Arg C_2 and DAK-Pto C_2). **A–E**, *Orogalago saintexuperyi* gen. et sp. nov.: DAK-Arg-102 (holotype), left M_2 in occlusal (A, stereopair), buccal (B), lingual (C), distal (D) and mesial (E) views. **F–J**, *Orolemur mermozi* gen. et sp. nov.: DAK-Pto-055 (holotype), right M^1 or M^2 in occlusal (F, stereopair), lingual (G), buccal (H), distal (I) and mesial (J) views. Images are renderings of 3D digital models of the fossil specimens, obtained by X-ray micro-computed (µCT) surface reconstructions (segmented enamel surfaces). Scale bars = 1 mm.

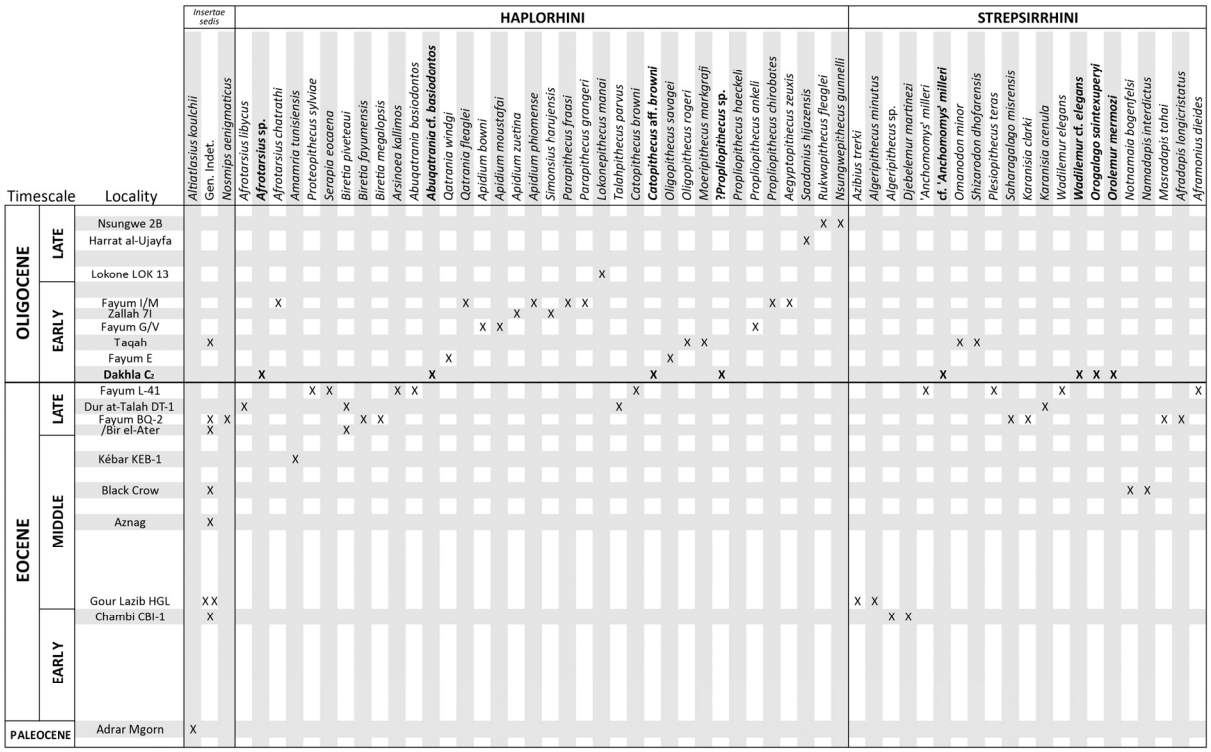

Figure 8. Temporal distribution of primates from the Paleogene of Afro-Arabia (modified after Seiffert, 2012, fig. 2). The temporal distributions of hystricognathous and anomaluroid rodents from the Paleogene of Africa are provided in Marivaux et al. (2017a, b).